Platone

PLATFORM FOR OPERATION OF DISTRIBUTION NETWORKS

Platone

PLATform for Operation of distribution NEtworks

D5.4 v1.0

Use Case 1 Demonstration Report

The project PLATform for Operation of distribution NEtworks (Platone) receives funding from the European Union's Horizon 2020 research and innovation programme under Grant Agreement no 864300.

Project name	Platone
Contractual delivery date:	31.08.2021
Actual delivery date:	25.08.2021
Main responsible:	Benjamin Petters, Avacon Netz GmbH
Work package:	WP5 – German Demo
Security:	P = Public
Nature:	R
Version:	V1.0
Total number of pages:	64

Abstract

This document describes the first results, lessons learned and conclusion of the application of Use Case 1 of the German Demo in Platone.

Keyword list

Islanding, Smart Grids, Energy Community, Battery Storage, Local Balancing

Executive Summary

Innovation for the customers, innovation for the grid" is the vision of project Platone - Platform for Operation of distribution Networks. Within the H2020 programme "A single, smart European electricity grid", Platone addresses the topic "Flexibility and retail market options for the distribution grid". Modern power grids are moving away from centralised, infrastructure-heavy transmission system operators (TSOs) towards distribution system operators (DSOs) that are flexible and more capable of managing diverse renewable energy sources. DSOs require new ways of managing the increased number of producers, end users and more volatile power distribution systems of the future. Platone is using blockchain technology to build the Platone Open Framework to meet the needs of modern DSO power systems, including data management. The Platone Open Framework aims to create an open, flexible and secure system that enables distribution grid flexibility/congestion management mechanisms, through innovative energy market models involving all the possible actors at many levels (DSOs, TSOs, customers, aggregators). It is an open source framework based on blockchain technology that enables a secure and shared data management system, allows standard and flexible integration of external solutions (e.g. legacy solutions), and is open to integration of external services through standardized open application programme interfaces (APIs). It is built with existing regulations in mind and will allow small power producers to be easily certified so that they can sell excess energy back to the grid. The Platone Open Framework will also incorporate an open-market system to link with traditional TSOs. The Platone Open Framework will be tested in three European field trials and within the Canadian Distributed Energy Management Initiative (DEMI)."

In WP 5 of the Platone project, Avacon with the support of the consortium, has conceptualized, implemented and successfully integrated a decentralized Energy Management System (EMS) prototype, named Avacon Local Flex Controller (ALF-C), into a bounded low-voltage grid section. The ALF-C is an EMS that provides decentralized SCADA / ADMS functionalities for DSO, TSO and customers. The principle of the ALF-C follows the edge computing paradigm. Its functionalities create more transparency of the generation, consumption and status of a bounded low voltage grid section and implements a local balancing mechanism for a large number of small scaled flexible assets for monitoring and control.

With the help of the ALF-C, the increasing number of dormant untapped flexible assets located in LV-networks, e.g. battery storage, shall be integrated into an active, decentralized grid management in order to increase the share renewable energy in distribution networks and reduce power peaks to make operation of the electricity distribution network more efficient. As part of the field test, Avacon targets the investigation of the network recuperation of an exemplary future low-voltage network and energy community practicing collective self-consumption. In addition, the technical feasibility of use of flexibility located in the bounded low voltage grid section / energy community shall be demonstrated and the effect evaluated.

The demonstrator has been implemented in a representative grid section that already today represents the expected generation and consumption characteristics of future low-voltage networks. The field test area consists of approx. 90 households with a high proportion of generation from roof-top photovoltaic systems. A central battery storage system was integrated into the area, which simulates the future storage capacity of household battery storage systems and electric vehicles. With the given field test setup, first tests with UC 1 were carried out. The target set were, on the one hand, testing the technical requirements for UC 2 to 4 and, on the other hand, the examination of network perturbations of an energy community that practices energy sharing for collective self-consumption. As part of the use case, local self-consumption shall be maximized and the power exchange at MV-feeder minimized. In the first release of the ALF-C prototype, a balancing mechanism with a soft real-time measurement control process with a cycle rate of 15 minutes was implemented.

After 6 months of measuring the net power and energy exchange at the MV / LV grid connection point and the first few weeks of application of UC 1, the following conclusions and results were collected:

1.) Communities with a high share of PV-systems located in bounded LV networks are rather energy producers, exporting energy, rather than consuming energy (importing).

2.) Communities with a high amount of installed PV power cause high-frequency power fluctuations at the medium voltage (MV) -feeder.

3.) The power consumption at night time at the MV-feeder shows characteristics of a standard load profile of a household, the power export on clear summer days shows the characteristics of the PV feeders (bell-shaped curve).

As part of the UC 1 application with the given field test setup the ALF-C enabled the local network to reduce a.) the peak value of power flow, b.) the energy exchange and c.) the amount of exported energy, and d.) lengthen the duration of the energetic decoupling from the MV-network. It was thus successfully demonstrated that the solution increased the community's self-consumption and relieved the MV network from additional stress. The inertia due to the delay in time of the readjustment of charging and discharging power of the local Battery Energy Storage System (CBES) has proven to be a bottleneck. The 15-minute measurement-control-cycle, in conjunction with the high frequency power flow fluctuation from PV system in daytime, sometimes lead to large consumption power peaks at the MV feeder. Even a weather forecast for the forecast of consumption and generation is not able to provide data with sufficient quality to forecast these short-term high frequency fluctuations. It further has been shown that the CBES with 777 kWh of storage capacity does not provide sufficient capacity to fully compensate intraday generation surpluses. In order to further reduce the peak power values at the MV feeder, the use of the limited available storage capacity must be optimized. With the help of an optimizer, the local balancing mechanisms shall enable the compensation of high midday generation peaks and increase local self-consumption simultaneously. This optimizer will be implemented and tested in upcoming releases. This functionality will build the foundation for the forthcoming application of UC 3 and 4 by month M31.

Authors and Reviewers

Main responsible		
Partner	**Name**	**E-mail**
Avacon Netz		
	Benjamin Petters	benjamin-georg.petters@avacon.de
	Navreet Dult	navreet.dult@avacon.de
	Christoph Jätz	christoph.jaetz@avacon.de
Author(s)/contributor(s		
Partner	**Name**	
RWTH Aachen		
	Amir Ahmadifar	aahmadifar@eonerc.rwth-aachen.de
Reviewer(s)		
Partner	**Name**	
ACEA		
	Gianluca Nori	
Engineering		
	Ferdinando Bosco	
Approver(s)		
Partner	**Name**	
RWTH Aachen		
	Padraic McKeever	

Table of Contents

1 Introduction

The project "PLATform for Operation of distribution Networks – Platone" aims to develop an architecture for testing and implementing a data acquisition system based on a two-layer Blockchain approach: an "Access Layer" to connect customers to the Distribution System Operator (DSO) and a "Service Layer" to link customers and DSO to the Flexibility Market environment (Market Place, Aggregators, …). The two layers are linked by a Shared Customer Database, containing all the data certified by Blockchain and made available to all the relevant stakeholders of the two layers. This Platone Open Framework architecture allows a greater stakeholder involvement and enables an efficient and smart network management. The tools used for this purpose will be based on platforms able to receive data from different sources, such as weather forecasting systems or distributed smart devices spread all over the urban area. These platforms, by talking to each other and exchanging data, will allow collecting and elaborating information useful for DSOs, transmission system operators (TSOs), Market, customers and aggregators. In particular, the DSOs will invest in a standard, open, non-discriminatory, blockchain-based, economic dispute settlement infrastructure, to give to both the customers and to the aggregator the possibility to more easily become flexibility market players. This solution will allow the DSO to acquire a new role as a market enabler for end users and a smarter observer of the distribution network. By defining this innovative two-layer architecture, Platone strongly contributes to removing technical and economic barriers achieve a carbon-free society by 2050 [1], creating the ecosystem for new market mechanisms for a rapid roll-out among DSOs and for a large involvement of customers in the active management of grids and in the flexibility markets. The Platone platform will be tested in three European trials (Greece, Germany and Italy) and within the Distributed Energy Management Initiative (DEMI) in Canada. The Platone consortium aims for a commercial exploitation of the results after the project is finished. Within the H2020 programme "A single, smart European electricity grid" Platone addresses the topic "Flexibility and retail market options for the distribution grid".

In Work Package 5 Avacon designs, develops and implements a decentralized Energy Management System (EMS), named Avacon Local Flex Controller (ALF-C), within a selected community's low-voltage grid. The ALF-C is an EMS that provides decentralized SCADA / ADMS functionalities for DSO, TSO and customers. The design of the ALF-C follows the edge computing paradigm. Core functionalities are the constant monitoring of the assets in the low-voltage grid and local balancing mechanisms to foster integration of renewable generation and increase the efficiency of existing networks.

The field test of Use Case 1 tests and evaluates the technical requirements for the following Use Cases 2-4 and examines of network perturbations of an energy community that practices energy sharing for collective self-consumption. The households, local photovoltaic system, battery storages and flexible loads of the community are connected the same low voltage grid section, described as a bounded grid section. The bounded grid section is connected to the MV-network along one MV-feeder. As part of the Use Case 1, local self-consumption shall be maximized and the power exchange at MV-feeder shall be minimized. In the first release of the ALF-C, a balancing mechanism based on a soft real-time measurement-control-cycle will enable a direct activation of flexibilities in cycles of 15 minutes.

1.1 Task 5.4

Deliverable D5.4 presents the results of Task 5.4. The aim of this task is to analysis how the demonstrator performed based on previously defined key performance indicators (KPIs). This analysis shows the technological impacts and benefits that the application of the smart grid architecture and control solution employed in this project has when applied to the considered use cases.

1.2 Objectives of the Work Reported in this Deliverable

The objective of this deliverable is to present the first results and experiences from the measurement of the net power and energy exchange of an energy community located in bounded low-voltage grid as well as the results of the Use Case 1 testing applied with the first release of the ALF-C prototype. Based on the collected results the implication on future operation are determined.

1.3 Outline of the Deliverable

The second chapter of this document gives a short summary of the objectives of WP 5 ALF-C prototype and Use Case 1. The third chapter describes the legal and regulatory background for Use Case 1 and the use of flexibility. The following chapter 4 provides an overview of the field test setup. Relevant data collected for Use Case 1 are described in chapter 5. The results of the measurement of the community power and energy exchange with the MV network without the application of Use Case 1 are described in Chapter 6. The measurement results after UC 1 application are described in Chapter 7. Chapter 8 gives an evaluation of KPIs. Chapter 9 describes the lessons learned. Finally, Chapter 10 concludes this deliverable

1.4 How to Read this Document

This document provides relevant experiences and lessons learned from the use case demonstration.

A first draft of concept of the solution design and technical specification of the architecture is provided in D5.1 [2]. A detailed description of use cases and KPIs for the evaluation of the use case data and measurement results is provided in D5.2 [3]. However, changes towards KPIs are described in this deliverable. Further KPI are defined in D1.2 [4]. More information about the dependencies of this work package with the others is described in D9.4 [5]. Further information about relevant legal and regulatory aspects can be read in D1.3 [6].

2 Motivation and Objectives

Use Case 1 aims to enable citizens located in a selected field test region to practice collective self-consumption by using available flexibility from battery storages. The collective self-consumption requires the synchronization of generation from local PV with available battery charging by an Energy Management System (EMS) developed as part of Platone and named Avacon Local Flex Controller (ALF-C). The trial is implemented in a local low-voltage grid section located in a rural region, that is representative for future citizen energy communities and renewable energy communities, consisting of private agricultural buildings, customer households with privately owned flexible loads, storages and photovoltaic generators. The Use Case 1 targets the investigation of different approaches of a local balancing mechanism the generation and consumption behaviour of future energy communities. Specifically, the net power and energy exchange at the grid connection point (MV-feeder) shall be examined and minimized during the Use Case 1 application.

Increase DER, Generation Capacity, Fluctuation

Today, distribution grids are already challenged by the high amount of fluctuating feed-in from DERs connected to the MV grid. Even in low-voltage levels (LV) of the distribution network, the amount of generation and demand increasingly leads to additional stress on MV grid lines and feeders. These challenges result from the increasing number of privately-owned small-scaled generators such as roof top photovoltaic (PV) systems and small-scale flexible loads such as heat pumps connected to LV grids. In future, the challenges will increase since more and more households will own a roof top PV system. At the same time, the load demand in LV grids will rise as a result of the increasing share of electric vehicles in the mobility sector, that require charging stations connected to LV grids. Additionally, oil heaters will be replaced by heat pumps, coupling the power and heat sector.

Energy Communities as Source of Flexibility

The EU entails a transition to a low-carbon energy system in which renewable energy sources (RES) play an important role and new technologies are developed and implemented. The EU sets the customer at the heart of the energy transition and some of them are already playing an active role, for example in the production of renewable energy or the management of local networks. The Renewable Energy Directive 2018/2001 (REDII) [7] and the recast Internal Market Directive 2019/944 (IMD) [8] establish a supportive legal framework for energy communities. Those communities can create great value and help citizens become more actively engaged in the energy transition. DSOs have a key role to play in enabling their proper development and integration into the distribution network. Communities in future will generate, distribute, consume, store, sale, aggregate, supply and share renewable energy. The large amount of flexible resources located within the community can be offered to the DSOs, Transmission System Operator (TSO) or Supplier / Balance Responsible Party (BRP) who can then use it for their needs. Strong cooperation between energy communities and system operators is therefore essential to ensure that this new type of actor will contribute to the stability of the whole energy system by allowing it to offer its flexibility. The collaboration between energy communities and DSO can have benefits for the transition of energy system:

• Source of Flexibility: Customers have a valuable source of flexibility for the energy system, adjusting demand patterns to system needs, which is needed in the future where we anticipate an energy system that is mainly based on volatile renewable energy sources and that is highly electrified.

• Aggregation and Optimization: An interface between DSO and communities can be realized behind energy communities that can aggregate and optimise their supply and demand. This optimization in conjunction with DSOs should make a positive contribution to the overall efficiency level of the energy system as opposed to building parallel infrastructures when there is little or no coordination/cooperation.

• Improved Quality of Supply: The expected flexibility within an energy community will support both the quality of electricity supply within the community itself as well as for the area surrounding it. Especially for isolated areas in which the connection to the grid is subject to uncertainties, for instance for islands connected with subsea power lines, the implementation of an energy community combined with a grid connection increases the quality of supply.

Objective

Avacon targets to implement an interface between a community and the DSO in order to simulate a collaboration. The ALF-C as local EMS provides local balancing mechanisms that, within Use Case 1, enables a community collective self-consumption and reduces the load and energy exchange along the MV/LV grid connection point and thus energetically uncouples them from the feeding MV-network ("Virtual Islanding").

The balancing mechanism will enable the EC to maximise consumption of locally generated energy and reduce power peaks at the LV/MV grid connection point. During the application of Use Case 1 the effect of load flow changes of a LEC on the MV grid and balancing functionalities that are prerequisite for Use Case 2, 3 and 4 shall be examined. The Use Case has been implemented in two steps with different functional principles of the balancer. More information about Use Case (UC) 1 – Virtual Islanding can be found in Platone deliverable D5.2 [3] and Platone deliverable D1.1 [9].

3 Legal and Regulatory Context

3.1 General Guidelines for Connection of RES for DSO

The renewable energy act ("Erneuerbare Energien Gesetz" or "EEG" [10]) in §12 states that grid operators are obliged to connect all sources of renewable energy to their network at request and ensure that their network offers enough hosting capacity to accommodate all energy that is produced under the EEG. This includes the obligation to optimize, expand and reinforce the network whenever necessary. The Energy Industry Act ("Energiewirtschaftsgesetz" or "EnWG" [11]) additionally claims in article 11.1 that the DSO as operator of energy supply networks are obliged to operate, maintain and optimize, strengthen and expand a safe, reliable and efficient energy supply network without discrimination, as far as it is economically reasonable.

3.2 Legislation on Renewable Energy Community

The guideline for a legislation on Renewable Energy Communities, as targeted in Use Case 1, is described in the Directive (EU) 2018/2001 on the promotion of the use of energy from renewable, which describes in Article 22 No 2 (a) that Member States shall ensure that renewable energy communities are entitled to produce, consume, store and sell renewable energy, including through renewables power purchase agreements" and in (b) „ share, within the renewable energy community, renewable energy that is produced by the production units owned by that renewable energy community" [7].

At the time of writing this deliverable, there was no ratified legislation or regulatory requirement in Germany that explicitly implements the above-mentioned requirement of the Directive (EU) 2018/2001 [7]. The German Civil Code ("Bürgerliches Gesetzbuch" or "BGB") offers an approach for a legal basis. In §705 of the German Civil Code the German legislation foresees guidelines about the formation and responsibilities of private individuals that form a joined company under civil law, the set guidelines are partially implemented here.

3.3 Legislation towards Energy Management Operation

To enable a community to share energy, an energy management system is required that implements local balancing mechanisms in order to synchronize generation and consumption with the help of storage facilities in such a way that the self-consumption of locally generated energy is maximized and the use of flexibility is minimized. Use Case 1 targets to implement such a mechanism and test it within the demonstration phase. The current laws do not provide an explicit regulation as to whether such an energy management may be operated by the DSO, TSO or others. The German regulation imposes in the energy industry act (EnWG), in the paragraphs §§ 6, 7, 8, 9, a general legal requirement for a separation (unbundling) of grid operation by DSO and TSO and sales activities by energy supply companies. The aim is to ensure neutral network operations.

The current law excludes the DSO from the operator role of the EMS. However, with the increasing installed capacity of RES generators integrated into the distribution network the need for technologies that enable more efficient operation of the distribution network increases. The active control of flexible loads and storages is one major technical solution. The mechanisms for flexibility activation will be market-based (e.g. flexibility markets) or will take place via direct control by the DSO. For both variants, the legal framework has not yet been implemented or sufficiently implemented into German legislation to make maximum use of the existing potential for flexibility that is already available. The following section describes the relevant legislation for Use Case 1 set by the EU and German legislation.

3.4 Legislation towards Direct Flexibility Mechanisms for DSOs

RES feed-in curtailment

If the grid capacity is temporarily insufficient, §14 EEG enables a curtailment mechanism which allows grid operators to temporarily reduce the feed-in by DER to maintain a safe and stable operation. When curtailments are carried out, owners of DER qualify for financial reimbursements which are recovered via the grid operator's grid charges. The obligation to increase grid capacity remains, nonetheless.

In practice this curtailment mechanism is triggered when a grid operator identifies a critical situation and has exhausted all other options to bring the network back to normal. TSO and DSO can trigger the mechanism alike, if the TSO owns the congestion it can request the underlying DSO to reduce feed-in on relevant lines and substations accordingly. Common scenarios to trigger a curtailment are for example:

• Overload of power lines in the VHV system

• Overload of transformers connecting HV and VHV networks

• Overload of power lines in the HV system

• Overload of transformers connecting HV and MV networks

The curtailment mechanism is rarely triggered by events below the HV/MV-substation due to lack of monitoring and control capabilities in these networks.

Windfarms and large photovoltaic generators are equipped with a controller and a radio receiver for ripple control signals. The ripple control allows grid operators to limit feed-in in four discrete setpoints, it can limit the generator to 0%, 30%, 60% or 100% of its nominal power output. Since the technology requires additional technical components to be implemented at generator premises, owners are facing additional costs for the equipment and service. In low-voltage networks, where installed capacities of generators are low and the installation of a ripple control might lead to disproportionately high costs, customer have the choice to implement a static limiter, that limits the feed-in to 70% of the installed generation capacity. The limiter is implemented in the inverter of the photovoltaic system.

Demand Response

The directive 2012/27/EU art 15 (4) states that « Member States shall ensure the removal of those incentives (…) that might hamper participation of demand response, (…) » as well as improving customer participation in demand response [12]. In Germany we find these aspects reflected in §14a Energy Industry Act (EnWG), which states that "Network operators are obliged to offer a discount on grid charges for those customers who offer controllability and flexibility to the system operator". It further states that the details of this controllability and flexibility scheme remains to be defined in a statutory law which is yet to be finalized. Until then however, a number of historic flexibility- and control-mechanisms have been grandfathered in under EnWG §14a.

The most common among these historic control mechanisms is a DSO-controlled switching of storage heaters that once applied to double-tariff customers. This kind of customer would receive a discounted energy tariff during off-peak hours. These tools were conceived in an era before the German energy system underwent unbundling, so back then the discount would apply on a combined retail and grid charge price. The distribution company would determine the discount and retain control over the definition and switching of peak and off-peak windows. Today retail and grid are unbundled so that the retail share of a customer's energy does not necessarily reflect the old double tariff model. However, under §14a EnWG the grid operator is still granting a grid charge discount in exchange for controllability and is still using the same systems to carry out the tariff switching, even though it might not have any effect on the retail side. The contractual agreement states that the DSO defines preferred charging times, guaranteeing a sufficient number of hours to cover customers energy demand. In practice, DSO usually have fixed charging windows during the night that amount to 8 hours of charging time. During these hours the customers heating device would charge up with thermal energy and release the heat throughout the following day. On particular cold days and in some regions, DSOs might also activate heaters for additional heating periods during the day to cover high demand.

Heat pumps on the other hand have not been around when the first installation of the double-tariff scheme took place in the 60s and 70s, so they are less burdened with historic flexibility mechanisms. Taking into account customer's expectation for comfort and the capabilities of the devices, today's agreement between DSO and customer under §14a EnWG states that Avacon has the right to interrupt the heat pumps operation for up to 2 hours, up to 3 times per day.

3.5 Market-Based Flexibility

The Electricity directive EU 2019/944 [8] on common rules for the internal market for electricity and amending Directive 2012/27/EU [12] describes that "Member States shall provide the necessary regulatory framework to allow and provide incentives to distribution system operators to procure flexibility services, including congestion management in their areas, in order to improve efficiencies in the operation and development of the distribution system. (Art. 32.1). The Internal Market Directive makes the basic decision that this flexibility is to be obtained in the market. The regulation has not been implemented into German legislation by now. However, a draft of an updated EnWG foresees it in article 14c.

4 Field Test Design

In the following chapter all relevant components that have been involved in the Use Case 1 demonstration will be presented in detail.

4.1 Field Test Area

The field test is located in Abbenhausen, a small village in the municipality of Twistringen in northern Germany. The community consists of about 90 households living in detached households. 16 buildings feature photovoltaic modules fixed to their rooftops. Additionally, three agricultural buildings are located in the region. All generators and loads of residents are connected to a LV-grid fed by a single smart secondary substation (MV/LV feeder). This region was selected as it fulfils multiple criteria. Firstly, the small village is very representative for communities in Avacon's service grid, which covers rural areas and offers huge potential for renewable generation. Secondly, the village is characterized by a high share of households owning a rooftop photovoltaic system, able to generate enough energy to be self-sufficient for several hours. Further details about the community are described in D 5.3 [13].

4.2 Relevant Actors and Components of Use Case 1

The following section gives an overview of relevant components for the Use Case 1 field test application. Further specifications on individual components are provided in WP 5 Platone deliverable D5.3 [13].

4.2.1 Rooftop Photovoltaic Modules

In Avacon's master data register for renewable energy producers, 16 grid connection points for rooftop photovoltaic systems are registered. The total installed generation capacity amounts to 302 kWp. A photo of Abbenhausen with its rooftop photovoltaic systems can be seen in Figure 1 where PV modules are highlighted.

Figure 1: Field Test Region with indication of Roof-Top Photovoltaic Systems

4.2.2 Smart Secondary Substation

The smart secondary substation, owned and operated by Avacon, accommodates a variable-frequency transformer that connects the community to the medium-voltage grid. The community is fed with energy from this single point. The substation is equipped with two measurement devices, each with a separate communication device. Measurement device 1 (right corner of Figure 2) is a PLMulti II, a standard measurement component, that is pre-installed in this type of substation. Measurement device 2 is a Phasor Measurement Unit (PMU), developed by RWTH Aachen. This device is installed in the top left corner, shown in Figure 2.

Figure 2: Smart Secondary Substation – Low-Voltage Connection to Bus Bar

4.2.3 Community Battery Energy Storage System

For the German demonstrator, Avacon has procured and installed a large-scale battery energy storage system (Community Battery System or CBES) manufactured by Rolls-Royce Solutions Berlin GmbH. The battery storage is manufactured as a containerized system, that includes all necessary auxiliary components. The battery cells are based on lithium-ion technology. The system has an installed power of 300 kW and a nominal storage capacity of 777 kWh. However, due to the new state of battery modules, the actual storage capacity is 878 kWh.

Figure 3: Community Battery Energy Storage Prototype

Measurement Device 1 - PLMulti II

The PLMulti II is a digital panel measuring device connected to the busbar. The device has up to 12 measuring channels for current measurement and 4 measuring channels for voltage measurement (L1, L2, L3, N). It is used especially for the efficient and cost-effective monitoring and evaluation of electrical systems. The PLMulti II is especially designed for measurements in low-voltage distributions grids. An advantage of this device is the independent measurement of up to 3 three-phase or up to 12 single-phase measurements. The measurement data is stored on an exchangeable SDHC memory card as a table. Additionally, this device provides an integrated Modbus RTU interface for remote read out, which is used in this demonstrator. The extreme minimum and maximum values as well as the accumulated meter reading of the energy meter are also permanently saved in the internal EEPROM memory of the device and can be displayed. The device fulfils DIN 43700. It provides real-time and mean measurement data. The sensors, voltage and current dividers are located at the low-voltage bus bar. The device is a standard communication component, that is installed ex work in the used type of secondary substation.

Figure 4: PLMulti II - Measurement Device

Measurement Device 2 – PMU

The Phasor Measurement Unit is made for monitoring applications in distribution grids. The device was developed by RWTH Aachen. It is designed for a cost-efficient scalability in medium and low-voltage grids. The core component is a Raspberry PI (RPI) 3. It includes the communication libraries libiec61850 [1] to send and receive data messages in Sampled Value format, according to the standard IEC 61850-90-5, and the code to acquire the samples and calculate the synchro phasor, frequency and ROCOF.

The RWTH Aachen has developed a software library with a set of algorithms to calculate synchro phasors, frequency and ROCOF. The calculation of active/reactive power can also be done in addition. The measurements are then encapsulated in the Sampled Value (SV) messages and later into UDP-IP packets, as recommended by the IEC 61850-90-5 standard for PMUs. The RPI runs the operative system Raspbian, which can operate the open source libraries libiec6850 for applying the IEC 61850 standard. The messages are also sent via Open VPN to ensure encryption and authentication features. Another possible implementation is performed via MQTT, where the PMUs act as clients communicating measurements to a broker (an MQTT server) that collects the data. The LOCO PMU can exchange measurements via Ethernet, WIFI and wireless adapters such as 3G/4G modem devices.

The choice of components of the PMU, its assembling, testing and installation has been refined and upgraded with support of Avacon's vocational training unit in order conform to industry standards for a safe and reliable operation in the field.

[1] https://github.com/mz-automation/libiec61850

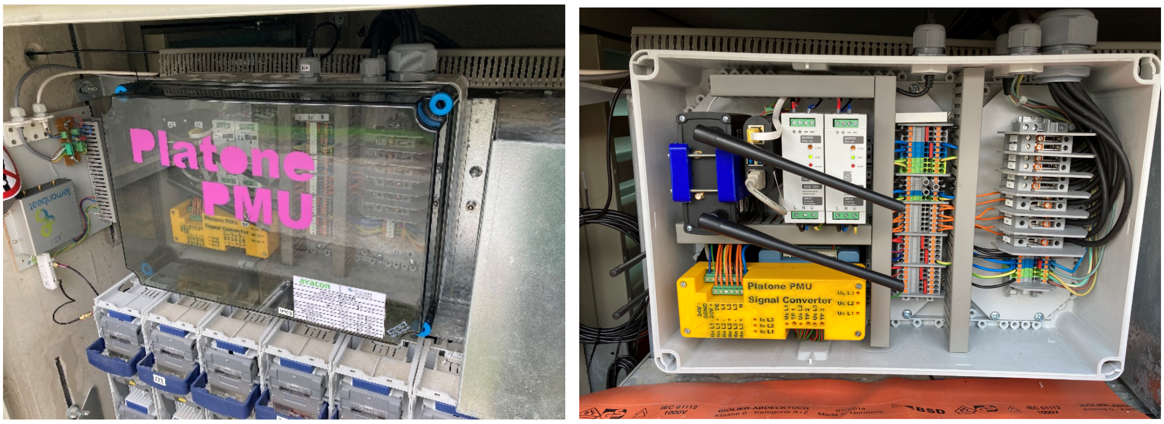

Figure 5: Phasor Measurement Unit with LTE Communication Device

4.2.4 Avacon Local Flex Controller (ALF-C)

The Avacon Local Flex Controller (ALF-C) is designed as a decentralized energy management system for the deployment of distribution grid services in low-voltage grids. It provides different functionalities for different use cases relevant to DSO, TSO, market participants or communities (CEC, REC). The system provides basic SCADA/ADMS capabilities and functionalities to monitor the grid state and to forecast generation and consumption to increase observation of individual LV grid section. It balances the local generation and consumption with direct control of small-scaled flexibilities of any type, such as battery storages and flexible loads, in response to violations of technical grid constraints or even external market signals. Within the application of four different use cases, the system will enable following functionalities:

- Monitoring of soft real time generation and/or demand,
- Forecasting of generation and demand,
- Local balancing of generation and demand in coordination with centralized grid management systems
- Within the use cases (UC) the ALF-C uses different algorithms to realise different targets:
- UC 1 the ALF-C targets to maximise self-consumption within LV network,
- UC 2 – Maintain a non-zero value defined for the power exchange at the grid connection point
- UC 3 & 4 – Enable energy supply and export of generation excess in bulks
- The ALF-C provides a set of features that are based on different functionalities implemented by algorithm developed and implemented with the support of RWTH Aachen.
- Data Visualization
- Data Storage for measurement, forecast and process data
- Local Balancing, State Estimation
- Forecasting

Local Balancing

Local balancing is a central feature for all use cases. The ALF-C aggregates flexibilities located in the community, balances the energy consumption with generation to achieve a specified net exchange target. For Use Case 1 three different mechanisms of the local balancing are implemented. Details of the algorithms are described in deliverable D5.3.

- **Soft Realtime Measurement-Control-Cycle Balancing**

  Local Balancing is a central feature for all Use Cases 1, 2, 3 and 4. It balances out the power consumption and generation to achieve specific targets with the help of flexible load and storages. For Use Case 1 three different mechanisms of the local balancing will be implemented. Details of the algorithm are described in deliverable D5.3 [13].

  With the help of this mechanism, the self-consumption within the community could be maximised in a soft-real-time manner. Furthermore, the peak power exchanges could also be avoided as long as the flexibility boundaries are satisfied. As soon as the flexibility boundaries, e.g., the maximum and minimum allowable state of charge for the storage units are deviated, the additional power generation and consumption should be exported and imported, respectively.

- **Forecast Based Control-Schedule Balancing**

  This balancing mechanism is based on a 24-hour forecast of the power exchange at the MV/LV grid connection point (community net load demand). The balancing mechanism is the same rule-based mechanism implemented for the soft real-time operation. However, unlike control-cycle balancing, a 24-hour set-point schedule is determined ahead of time based on the forecast data. Obviously, the same limitation with respect to reaching the flexibility boundaries exist in this mechanism since the control logic is a rule-based one. However, unlike the above-mentioned soft real-time mechanism, it could be predicted when and to what extent the flexibilities are utilised. This information could be used for other additional soft real-time mechanisms in which the flexibilities could be dynamically steered to avoid reaching the boundaries.

- **Forecast-Based Control-Schedule with Optimisation**

  Similar to the previous mechanism, the forecast-based control-schedule with optimisation balancing mechanism is based on the forecast data. However, instead of the rule-based control logic, the schedule set-points are computed using an optimisation technique. As the objective function, minimisation of the power exchange at the MV/LV is targeted considering the flexibility specifications and the corresponding boundaries. With the help of the optimisation, this mechanism can avoid peak-power exchanges in a more robust manner, since unlike the rule-based logic, the set-points are defined taking the whole forecast horizon and the limits of the storage flexibilities into consideration. In the rule-based approach, the power exchange at each instance of forecast horizon is balanced out irrespective of the power exchanges before and after this specific in-stance of time. Obviously, the performance of both balancing mechanisms (rule-based and optimization-based) depends on the forecast accuracy.

5 Relevant Use Case Data

5.1 Secondary Substation

The PLMulti II is installed in the secondary substation and provides 1-minute average values for:

- Active power P_{TEI} in kW
- reactive power Q in Vvar.
- voltage U in V
- current I in A
- phase angle in degree
- energy in positive direction, E+ in kWh (from MV to LV)
- energy in negative direction (E-) in kWh (from LV to MV)

The measurements are provided per phase (L1, L2, L3) and in total as sum of the measurements of L1, L2 and L3.

Active Power Exchange – (P_{TEI})

The measured total active power value data collected from the PLMulti II in the substation is one of the key quantities to evaluate Use Case 1. It shows the net-load of the LV-grid, i.e., the difference between consumption and generation. As an example, Figure 6 visualizes a 60 minutes period of the active power. The diagram shows one value per minute, in total 60. Positive values indicate an active power flow from the medium-voltage grid into the low-voltage grid. This is the case in times the total active power consumption is higher than the total generation. Negative values are caused by an active power flow from the low-voltage grid into the medium-voltage grid, i.e., when the generation is higher than the local demand.

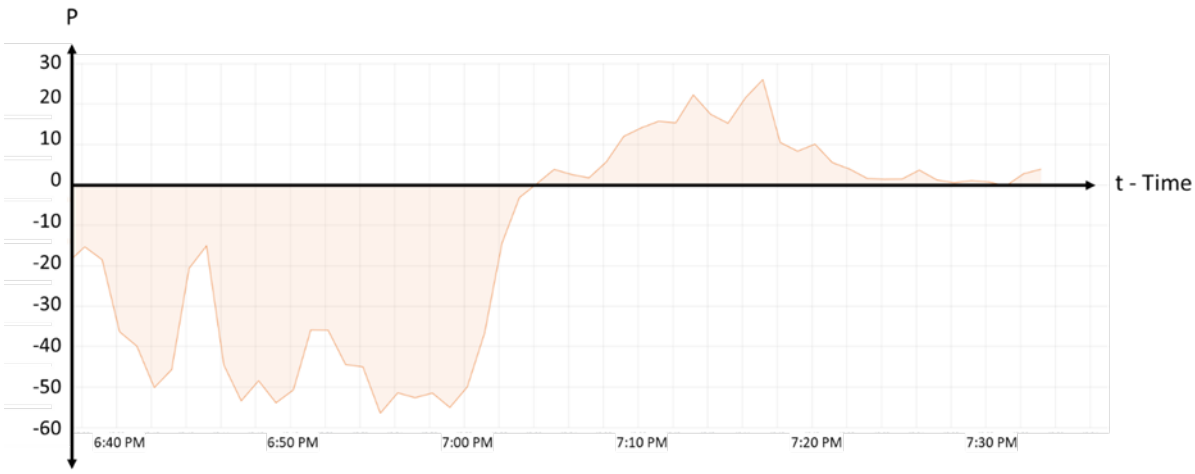

Figure 6: Example of 1-Minute Values of Active Power Measurement

Energy Exchange - (E_{TEI}, +, E_{TEI}, -)

The values for energy exchange at the MV/LV-grid connection point are stored in separate registers of the PLMulti II. One register continuously accumulates the energy flow from MV-grid into the LV-grid (E_{TEI}, +). Hence, E_{TEI}, + is the net energy demand. Conversely, the second register continuously accumulates the energy flow from LV-grid into the MV-grid (E_{TEI}, -), which is the net energy surplus that is exported.

5.2 Community Battery Energy Storage

State of Charge – (SOC)

The Community Battery Energy Storage (CBES) state of charge (SOC) is the state of charge of the CBES as a percentage value of its storage capacity. A value of 80 % indicates that 20 % of the currently available storage capacity are unused and available for charging.

State of Energy – (SOE)

The CBES state of energy (SOE) is the amount of energy in kWh that has been charged by the battery and is available for discharging.

Active Power – (P_{TCB})

P_{TCB} is the value of active power exchange between the battery and the LV-grid. A positive value indicates discharging and a negative value indicates charging of the CBES.

5.3 ALF-C

Forecast Active Power Exchange ($P_{F,\ TEI}$)

Use Case 1 includes a forecasting module that computes P_{TEI} for the next 24 hours based on a forecast of PV generation and household consumption.

Standard load profiles (SLP) are characteristic active power load profiles for different types of consumers of electricity. It captures the average change of active power over a period of time, e.g. 24 hours. The SLP is used for forecasting and balancing when no measurements are available. It is a simplification, used in a wide area of the energy sector. For example, electricity sales and large energy traders make use of these profile to forecast the energy demand for the relevant customer segment and to procure energy on the energy market without creating significant imbalances between generation and consumption. For this purpose, consumers or generators (customers, machines, factories, etc.) are grouped into clusters of characteristic load profiles. For Use Case 1 the standard load for households is used.

Setpoint - Active Power Exchange (P'_{TCB})

With its balancing module the ALF-C computes active power setpoints for the CBES to balance consumption with generation in such a way that P_{TCB} equals zero in Use Case 1. At a later stage in this project the available storage flexibilities will further include household battery storages. The upcoming challenge will be to disaggregate the setpoint for all aggregated storages in the community to each individual asset.

Calculated Active Power Exchange ($P_{C,\ TEI}$)

The calculated active power exchange P_C is a reference value that will computed ex-post when Use Case 1 was applied. This value represents a P_{TEI} that would have been measured if case Use Case 1 had not been applied. It is computed by adding P_{TCB} with P_{TEI}. It is an essential quantity that helps to evaluate the impact of the use cases on the balance of the LV-grid.

5.4 Example and Overview

The following example illustrates and explains the differences and meaning of the individual measured quantities P_{TEI}, P_{TCP} and P_C. The same format chosen for this example will be used again later for the Use Case 1 evaluations.

The following sample data ranges from June 3, 2021 at 3:50 p.m. to 8:00 p.m. the same day. In this example the application of Use Case 1 starts at 5:30 pm and last until the end. Figure 7 visualizes the measured active power exchange at the MV/LV grid connection point, P_{TEI}. From 3:50 PM to 5:30 PM Use Case 1 is not applied and the CBES is inactive (P_{TCB} = 0). At the beginning of the example the community is exporting energy, i.e., P_{TEI} < 0 because the generation of energy from PV modules is higher than the overall consumption. At about 5:00 PM P_{TEI} equals 0. At this point of time generation and consumption within the community are equal. After 4:50 p.m. the P_{TEI} fluctuates around 0 kW.

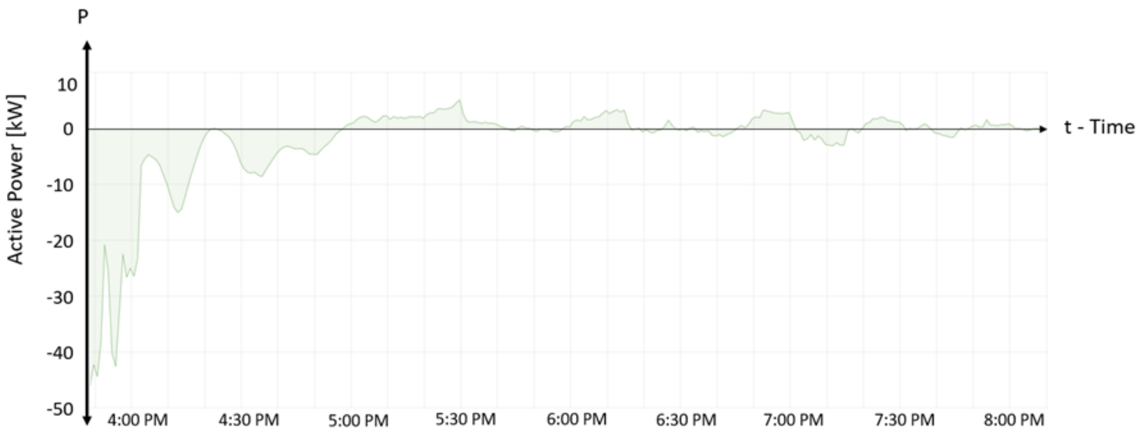

Figure 7: Example of P_{TEI}

At 5:30 Use Case 1 starts. The CBES is triggered by the ALF-C to discharge, which leads to a reduction of the active power exchange at the MV/LV grid connection point close to zero (P_{TCB} = 0). The red graph in Figure 8 shows that the battery is set to discharge with a value of about 20 kW (P_{TCB}) and increases step by step until 7 PM. Afterwards it decreases again. From 5:30 PM onwards, P_{TEI}, shown in green, is decreasing by about 20 kW. The blue line is the calculated power exchange at the MV/LV grid connection point (P_C) that would have been measured, if Use Case 1 would not have been applied. Figure 8 visualizes that from 4:50 PM to 5:30 PM P_C and P_{TCB} are of equal value. From 5:30 PM onwards P_C remains at about 25 kW as the battery begins to discharge and leads to a reduction of the measured power flow at the grid connecting point P_{TCB}.

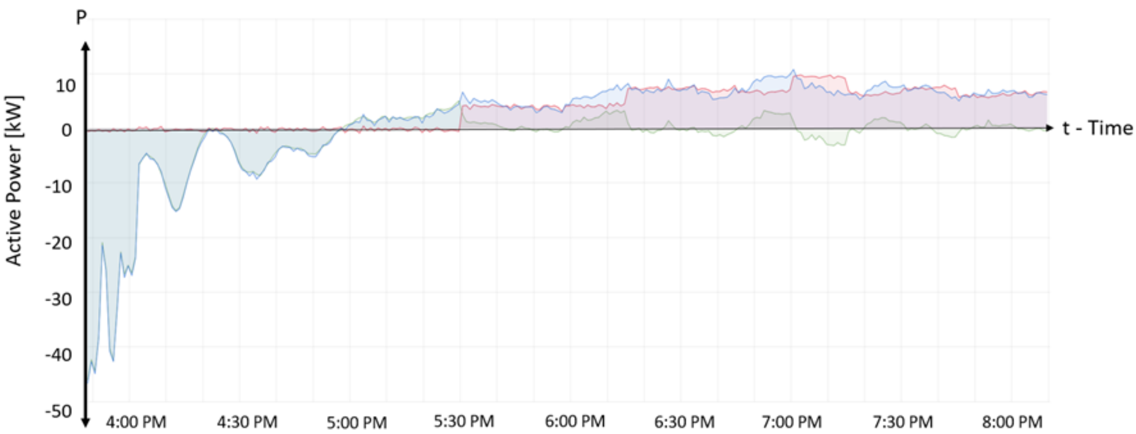

Figure 8: P_C and P_{TCB}

Table 1: Overview of Relevant Use Case Data

Place of Measurement	Value	Type	Indicator	Unit	Description
Secondary Substation	Active Power	Measured Value	P_{TEI}	kW	Community power exchange with MV network
Secondary Substation	Energy	Measured Value	$E_{TEI,+}$	kWh	Community net imported energy
Secondary Substation	Energy	Measured Value	$E_{TEI,-}$	kWh	Community net exported energy
ALF-C	Active Power	Forecast	$P_{F,TEI}$	kW	24-h forecast of community power exchange with MV network
ALF-C	Active Power	Setpoint	P'_{TCB}	kW	Setpoint schedule for CBES
ALF-C (Secondary Substation)	Active Power	Determined Value	P_C	kW	Calculated community power exchange with MV network if UC would not have been applied (P_{TEI}, no UC = $P_{TEI} - P_{TCB}$)
CBES	State of Charge	Measured Value	SOC	%	Relative state of charge (100% = 850 kWh)
CBES	State of Energy	Measured Value	SOE	kWh	Battery state of energy
CBES	Active Power	Measured Value	P_{TCB}	kW	Battery load (charging/discharging)

6 Results from Field Test Measurements

6.1 Energy Balance of the Community

Figure 9 shows the daily energy exchange measured at the secondary substation of Abbenhausen. As mentioned in the preceding sections, the measurement device PLMulti II has two separate registers for counting electric energy. The quantity $E_{TEI,+}$, i.e., energy import, is energy provided by the MV-grid when the demand for energy exceeds local generation. In the opposite case, when energy generation exceeds consumption, the energy $E_{TEI,-}$, i.e., energy export, is fed into the MV-grid. The energy balance is computed by taking the register value at the end of the day and subtract from it the register value at the beginning of the day. Thus, the daily energy balance is the average value for each day.

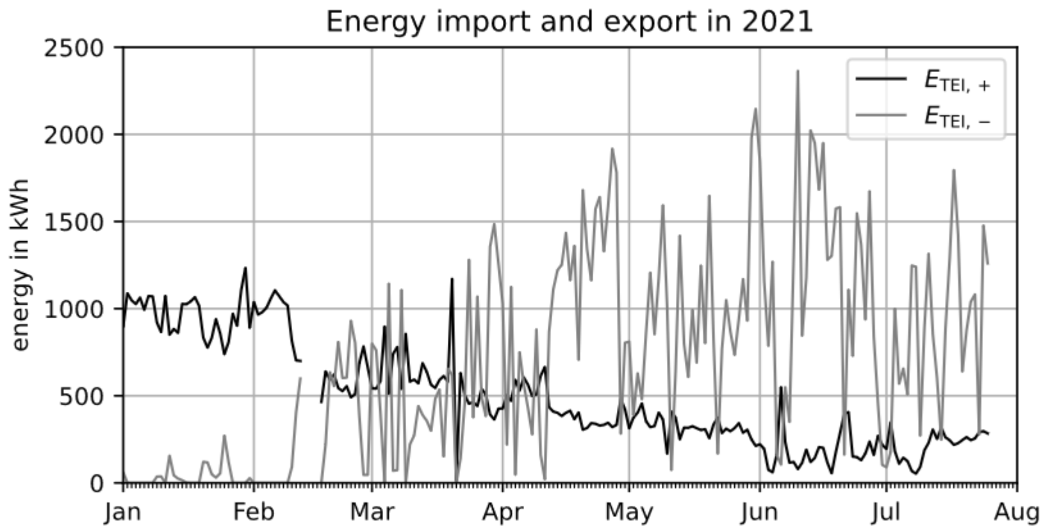

Figure 9: Import and Export of Energy into the Field Test Community

During the winter the miniscule generation of energy by the PV panels is not sufficient to satisfy the demand. The reason for this is likely a combination of short daylight hours, more cloud coverage and a lower zenith of the sun, resulting in more refraction of the light in the atmosphere and a disadvantageous incidence angle between the direct solar radiation and the PV panels fixed on the roofs. During these days, most of the energy consumed is provided by the MV-grid.

However, during the period beginning in the second half of February and lasting into April, there were occasional days on which the daily generation was larger than the daily consumption. After mid-April, as there were more clear days, more sunshine hours and better alignment between the PV modules and the sun. Additionally, the increase in daylight hours not only increases the potential for energy generation but *vice versa* decreases the night-time hours when energy must be provided by the MV-grid. This partly explains why there is a noticeable decrease in $E_{TEI,+}$ by a factor of four as the year progresses towards summer.

The difference ΔE_{TEI} between $E_{TEI,+}$ and $E_{TEI,-}$ is shown in Figure 10. Note that starting from April the community battery energy storage (CBES) was installed and connected to the LV-grid. Thus, when the CBES is active, it affects the energy balance of the community, e.g., reducing the energy export by storing the surplus energy and later reducing the energy import when discharging. By taking the change of state of energy of the CBES into account, it is possible to compute the energy difference for each day as if there had been no CBES, labelled $\Delta E_{TEI,c}$. Due to data transmission issues, $\Delta E_{TEI,c}$ is only computed for days where the state of energy for the CBES was unambiguous.

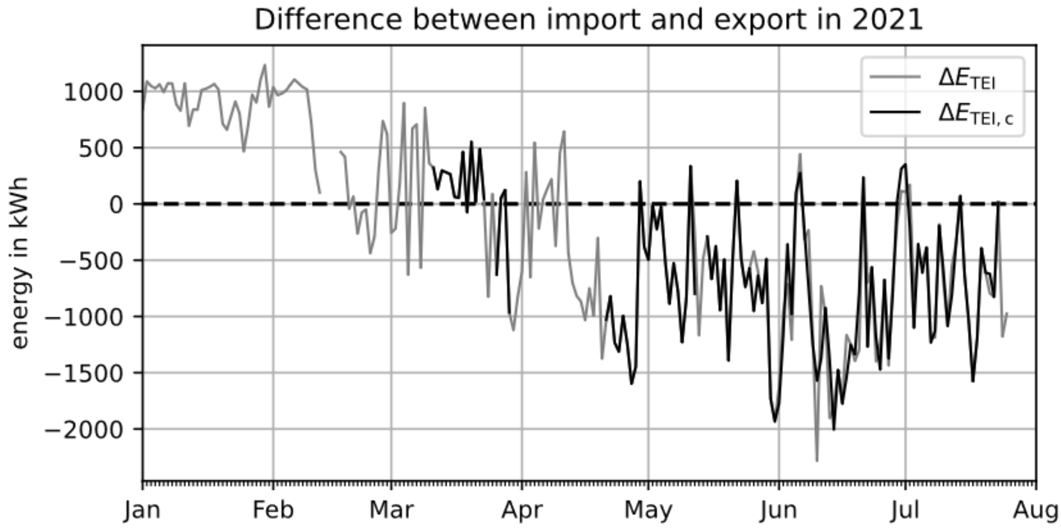

Figure 10: Difference between Energy export and import in the Field Test Community

Following the sign convention, negative values for ΔE_{TEI} are defined as an export of energy, i.e., the surplus generation from the PV modules is fed into the MV-grid. Respectively, a positive value for ΔE_{TEI} is defined as an import of energy to the community. Plotting the energy difference emphasizes the previous results; during winter the community depends on energy provided by the MV-grid while during summer the community could sustain itself if it could theoretically manage to store at least fractions of the surplus energy.

The apparent small difference between ΔE_{TEI} and $\Delta E_{TEI,c}$ has three causes. Firstly, UC 1 was only active for selected days. For days without UC 1, the state of energy of the CBES dropped only in small quantities due to self-consumption. Secondly, as expected in UC 1, most of the energy stored during the day is consumed within the following night. Thus, within the 24 hours span per sample, the reduction of $E_{TEI,-}$ during the day and $E_{TEI,+}$ during the night cancel each other out to some degree when computing the difference between them. Thirdly, for subsequent clear days the CBES operating in UC 1 is fully charged within a couple of hours and the demand for energy during the few night hours is not sufficient to fully discharge the CBES. Thus, on the following day the CBES has less available capacity and its impact on ΔE_{TEI} is limited. The latter two causes will be investigated in more detail for selected days in Ch. 7 of this deliverable.

It becomes apparent that if one would like the Energy Community to store all surplus energy generated in the summer to consume it during the following winter, and thus become fully energy independent, the size of the storage system would need to be of humongous proportions. For comparison, the CBES has a capacity of 777 kWh and thus would be too small to store even a single summer day of surplus energy generation! This demonstrates that the goal of local energy communities cannot be decoupling themselves from the electric grid. Instead, smart energy management systems — such as the ones implemented within the Platone project — are required to utilize all generated energy as economically as possible.

Another observation is the large volatility in energy export, hence generation by the PV modules. As seen at the end of April, within a couple of days a daily export of around 1,500 kWh can plummet to an import of around 200 kWh. This volatility between days prompts a more detailed analysis of the volatility over a single day as this has strong implications for the algorithms of the use cases.

Before this detailed analysis is presented in the following section, Figure 11 offers an alternative perspective on the daily generation of surplus energy. It shows the ratio of $E_{TEI,-}$ to $E_{TEI,+}$, i.e., how much more energy was exported than was required to import for each day. Note, that only days with no CBES interference are displayed to avoid ambiguity in the calculation of the ratio. It becomes evident that the community already exports up to eight times more energy than it requires to import. Overall, this ratio increases towards the summer. However, even a clear February day can generate a significant surplus of energy. The ratio, again, also illustrates the volatility in PV generation. The day of the highest production lies within a fortnight of the day of the lowest production during summer.

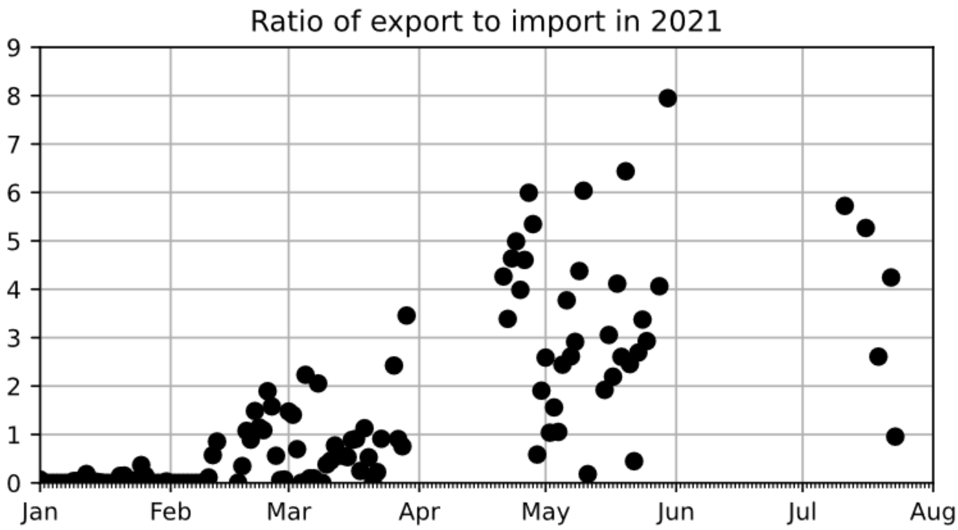

Figure 11: Ratio Energy Export to Energy Import

This investigation of the energy balance illustrates that a local community comprised of households and agricultural buildings, but without significant industry, can already generate as significant amount of energy — exceeding their own demand — using PV panels. The challenges that need to be addressed are managing the high volatility of the energy generation and using the energy as economically as possible, e.g., by storing it or feeding it into the MV-grid.

6.2 Influence of Weather Patterns on Daily PV Generation

In the preceding section, the daily energy balance throughout the first half of 2021 is investigated. This section continues with a more detailed analysis over single days. For this, three days are carefully selected with each day representing a distinct weather, i.e., cloud pattern: a clear and sunny day, a day with unsteady cloud coverage and an overcast day. The characteristics of each day is subsequently summarized in four plots.

The first plot of Figure 12 shows the power P_{TEI} measured at the secondary substation. The sign convention follows the convention established for energy — a positive sign denoting import and a negative sign denoting export. The reason for choosing power over energy for this analysis is that the power measurements feature a higher temporal resolution which is necessary when analysing the volatility of the solar power generation over a single day.

In addition to the measured quantity P_{TEI}, its average, $P_{TEI,mean}$, is shown in the first plot. The mean value was computed as a centred rolling average over 15 samples, i.e., minutes. The deviation from the mean for each point in time is shown in the second plot.

The third plot shows the minutes of sunshine for each hour. This shows the beginning and end of daylight hours as well as indicates the weather conditions on that day. The weather data was provided by the Deutsche Wetter Dienst (German Meteorological Service) [2] and accessed via the Python package offered by Meteostat [3]. The last plot is a histogram of the deviation from the mean value. Note that the time axis displays all times in UTC. On each selected day no ALF-C use case was active.

6.2.1 Clear Summer Day

Figure 12 shows the measured data for May 30, 2021. The power plot shows that during the night the community imports energy. Thus, P_{TEI} is a positive value with a peak value of 40.4 kW. However, as

[2] https://www.dwd.de/DE/Home/home_node.html
[3] https://github.com/meteostat/meteostat-python

soon as the sun starts rising, the PV panels produce enough power so that P_{TEI} becomes negative and energy is exported. Generation peaks at -261 kW around noon.

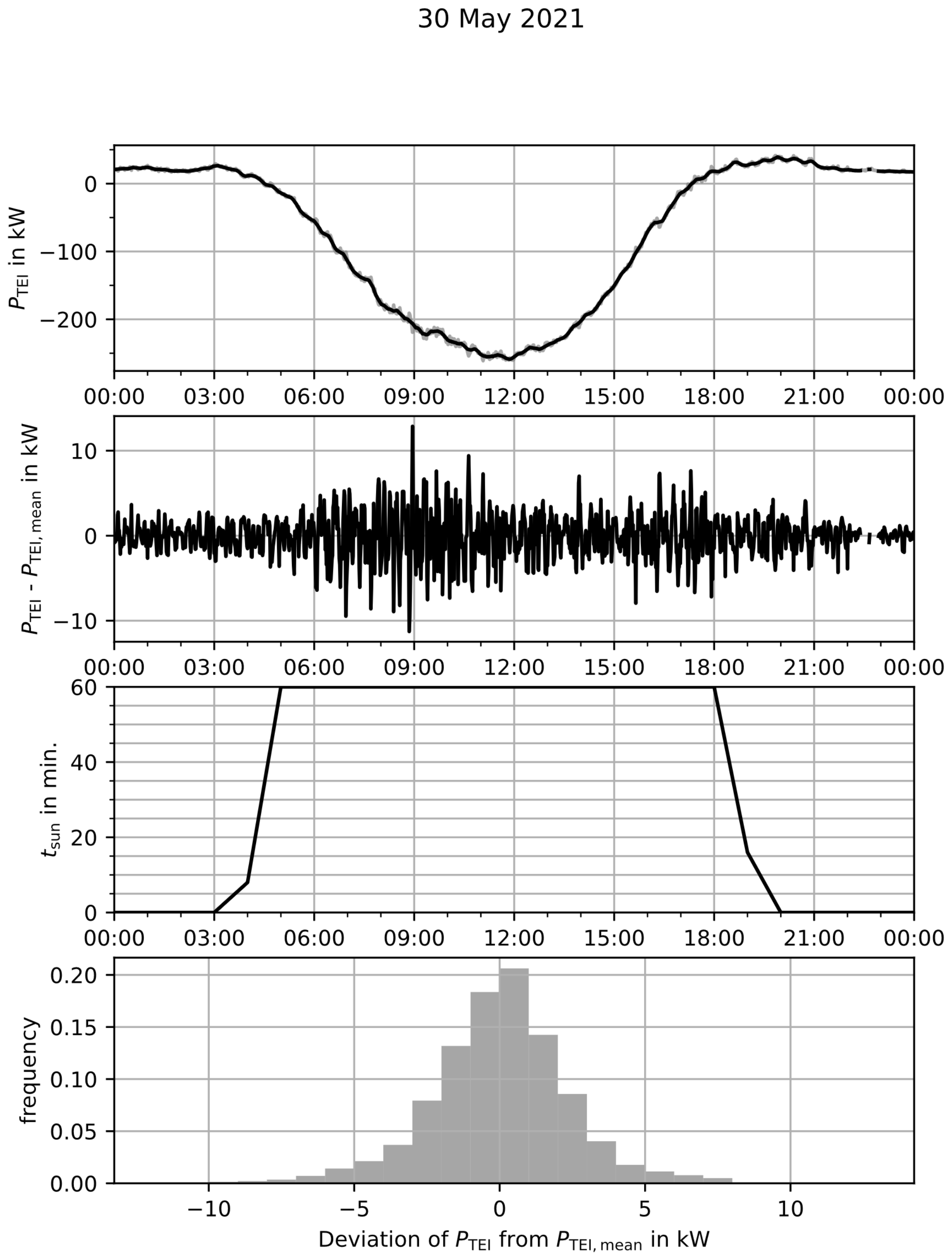

Figure 12: Power Characteristics of a Summer Day

Throughout the whole day, the shape of the power curve is very smooth. During the daylight hours, the deviation from the mean stays within 10 kW and is even less during night-time. It becomes apparent that on this day the community generated much more energy, given by the area under the P_{TEI} -curve, than it required. Indeed, the ratio of $E_{TEI,-}$ to $E_{TEI,+}$ for this day is almost eight, the highest value measured so far.

For such a clear day, it would be reasonable to expect that a properly sized energy storage system could provide enough energy during night-time hours so that no energy import would be required. For this particular day, the import demand at night was 250 kWh, less than one third of the capacity of the installed CBES. However, this would mean that the CBES will not completely discharge overnight thus having less capacity for the following day. This emphasizes the importance of the use cases UC 3 and UC 4 — investigated later in this field-test — which are defined respectively as scheduled charging from and discharging into the MV-grid.

Even though the CBES is capable to store energy for the night-time, its capacity is insufficient to store all the energy. This has a strong implication for the CBES control algorithm. While direct charging is easy to implement, it would charge the CBES completely within the morning hours. Alternatively, a forecast based peak-shaving would limit the feed-in into the MV-grid when it is highest — during noon hours.

6.2.2 Partly Cloudy Spring Day

Figure 13 shows the curve of P_{TEI} for a partly cloudy day in April that featured an unsteady weather pattern comprising alternating sunny and cloudy instances. Unlike on a sunny day, the curve is jagged and only smooth during night-time hours. The unsteady weather is also apparent in the sunshine per hour plot which implies an even split between instances of sunshine and cloud cover.

The alternating solar radiation results in steep gradients of power export; within the same hour, power can change by up to 250 kW. Additionally, the frequency of these changes in energy generation is below the frequency of the control cycle for UC 1 that currently is set to 15 minutes. This means that UC 1 with direct charging and discharging will be unable to compensate these fluctuations. Alternatively, the forecast-based approach could achieve reducing the average power export into MV-grid—including the fluctuations. The ratio of $E_{TEI,-}$ to $E_{TEI,+}$ for this day is about 3.4. While the fluctuations would make it challenging to store all the energy, it could be feasible to store enough to satisfy the demand for this day.

Another interesting observation is that the maximum export power, i.e., the minimum of P_{TEI}, is 299 kW. This is almost 40 kW higher compared to the sunny day in May analysed before. This is assumed to be a combination of two factors. Firstly, the lower zenith of sun on this day in April — 50 degrees compart to 60 degrees at the end of May — aligns better with most solar panels installed on the rooftops. This would allow to harness more energy from the direct solar radiation. Secondly, the energy generation of PV panels is highly sensitive to temperature; decreasing ambient temperature increases power output. The maximum temperature on this day in April was 9.5 degrees Celsius compared to 19.8 degrees Celsius on the sunny May day.

In summary, a day with unsteady weather patterns provides a formidable challenge to the energy management system. Even a faster control cycle might not be inadequate to compensate the fluctuations due to lag within the CBES control system and the additional stress the increase in charging cycles have on the longevity of the battery cells. However, despite the unfavourable conditions the community generated a significant amount of electrical energy on this day.

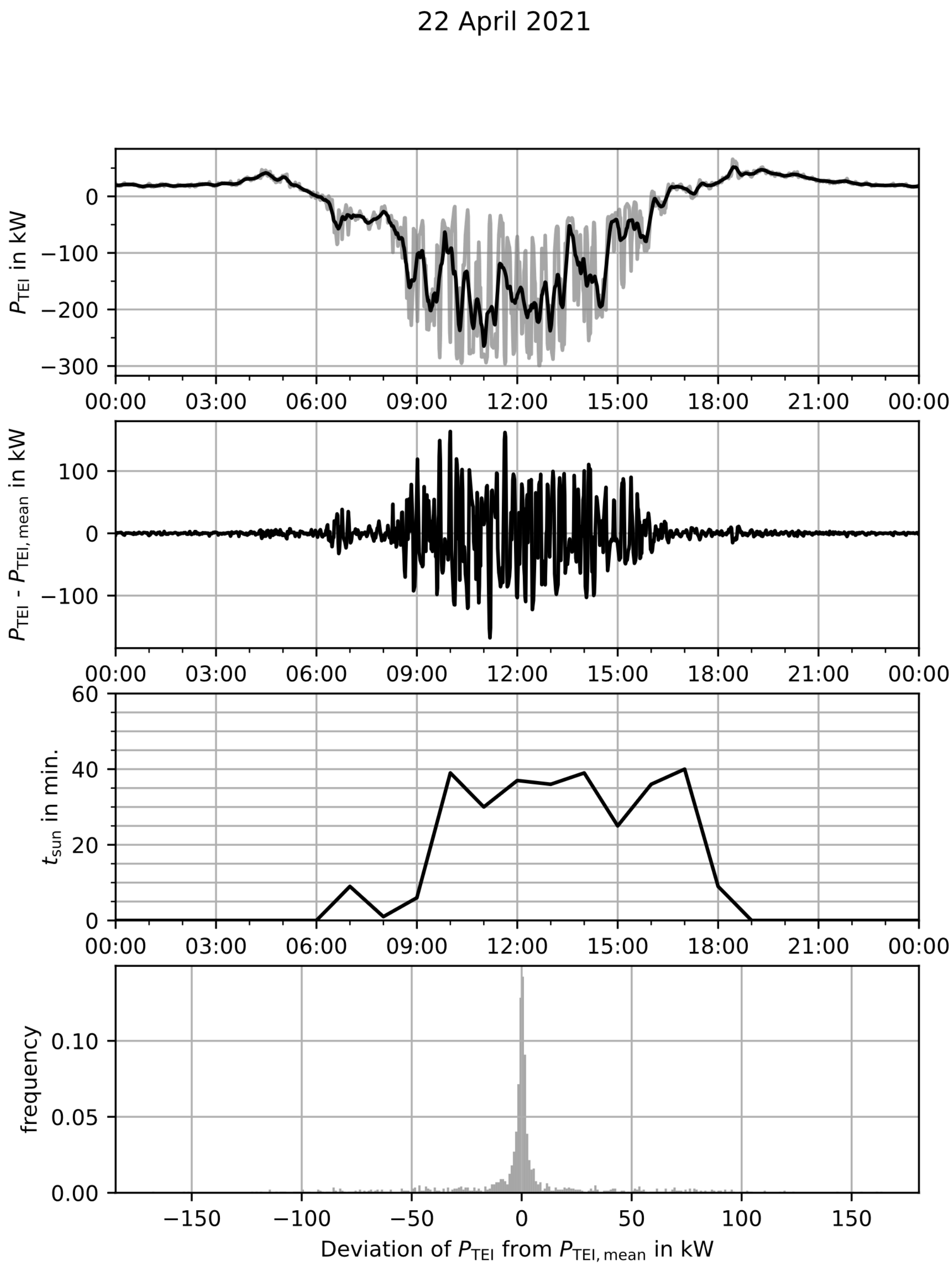

Figure 13: Power Characteristics of a Partly Cloudy Spring Day

6.2.3 Overcast Summer Day

The last example of a common weather pattern and its effect on the PV generation of the community is an overcast day from end of June, see Figure 14. Note, that the weather station did not recognize any sunshine for the whole day. The smoothness of the P_{TEI}-curves rests between the smooth sunny day and the jagged curve on a day with unsteady weather.

Except for two short peaks, the export of energy is significantly lower. Overall, the ratio of $E_{TEI,-}$ to $E_{TEI,+}$ is about 0.4 — for this particular day the community required energy import from the MV-grid or would have needed to store energy in the preceding days. This has implications for the energy management system. In the case of an overcast day with little energy generation, an optimization, based on accurate forecasts, would be required that decides between storing enough energy in the preceding days and importing energy from the MV-grid.

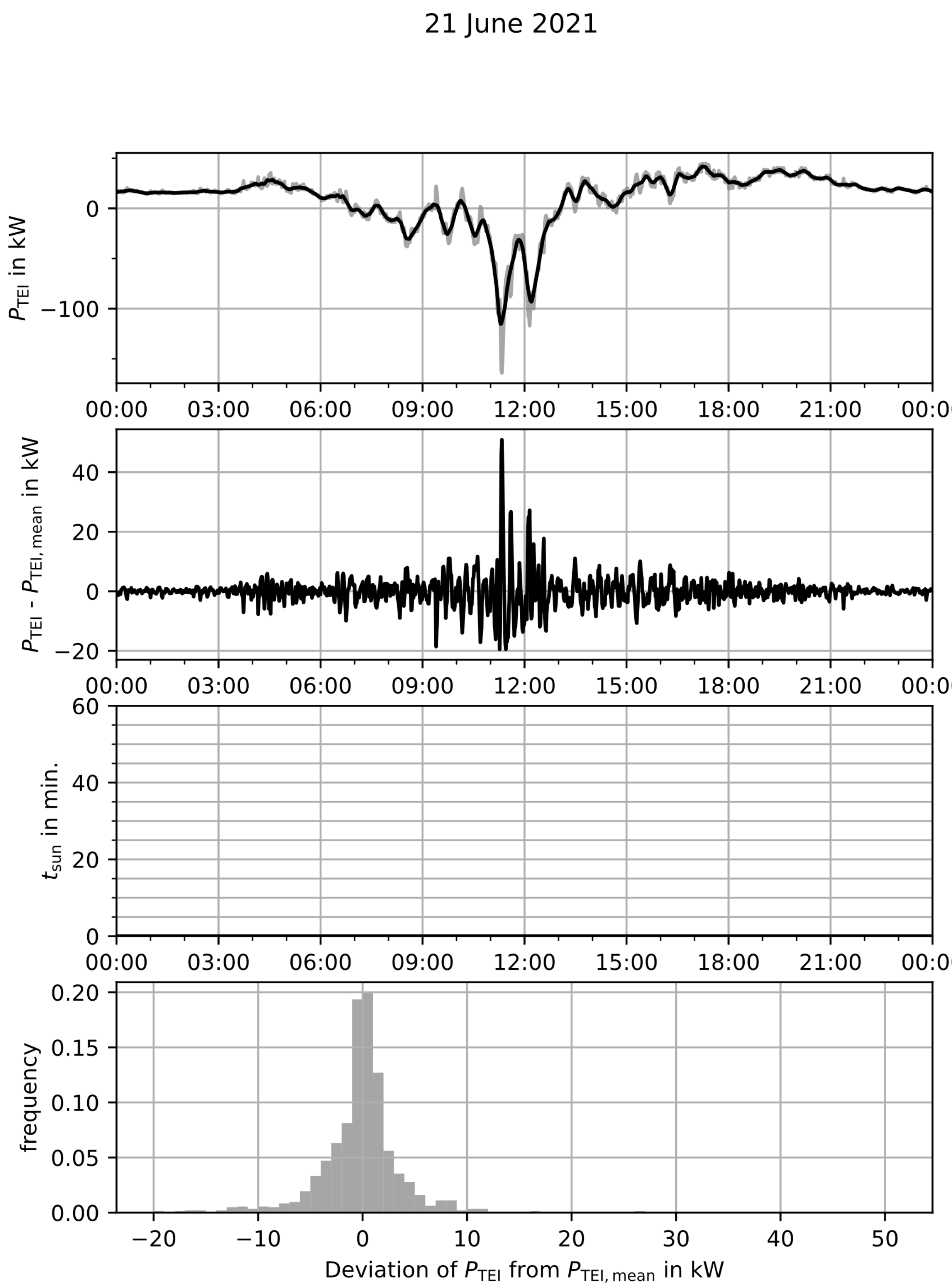

Figure 14: Power Characteristics of an Overcast Summer Day

7 Results of UC 1 Application

The results of the UC 1 application are evaluated for the period from June 30th 2021, 8:00 AM to July 6th 2021 0:00 AM. Within this period UC 1 has been applied for almost 139 hours starting from June 30 2021, 6:45 AM, to July 6th 2021, 0:00 AM. Table 2 indicates the status of the grid with relevant measurements at the starting point of UC 1. Table 2 and Table 3 give an overview of the values P_{TEI}, P_{TCB}, P'_{TCB}, P_C, and SOC for the period of investigation. The evaluation of results, characteristics and calculation of KPIs will be done for following periods:

Table 2: UC 1 - Evaluation Periods

UC 1 Evaluation Period	Period of Time	Duration
I	1/7/2021, 00:00 a.m. – 1/7/2021, 11:59 p.m.	24 h
II	2/7/2021, 00:00 a.m. – 2/7/2021, 11:59 p.m.	24 h
III	3/7/2021, 00:00 a.m. – 3/7/2021, 11:59 p.m.	24 h
IV	4/7/2021, 00:00 a.m. – 4/7/2021, 11:59 p.m.	24 h

Status at UC 1 -Start

The following table display the status at the beginning of the UC 1.

Table 3: Status of the grid at point of UC 1 Start

Indicator	Value	Notes
P_{TEI}	29,3 kW	
$E_{TEI,+}$	149,973 kWh	
$E_{TEI,-}$	126,000 kWh	
P'_{TCB}	0 kW	
P_C	28,3 kW	
SOC	49 %	SOE (SOC = 100%) = 879.98 kWh
SOE	431,19 kWh	
P_{TCB}	0 kW	

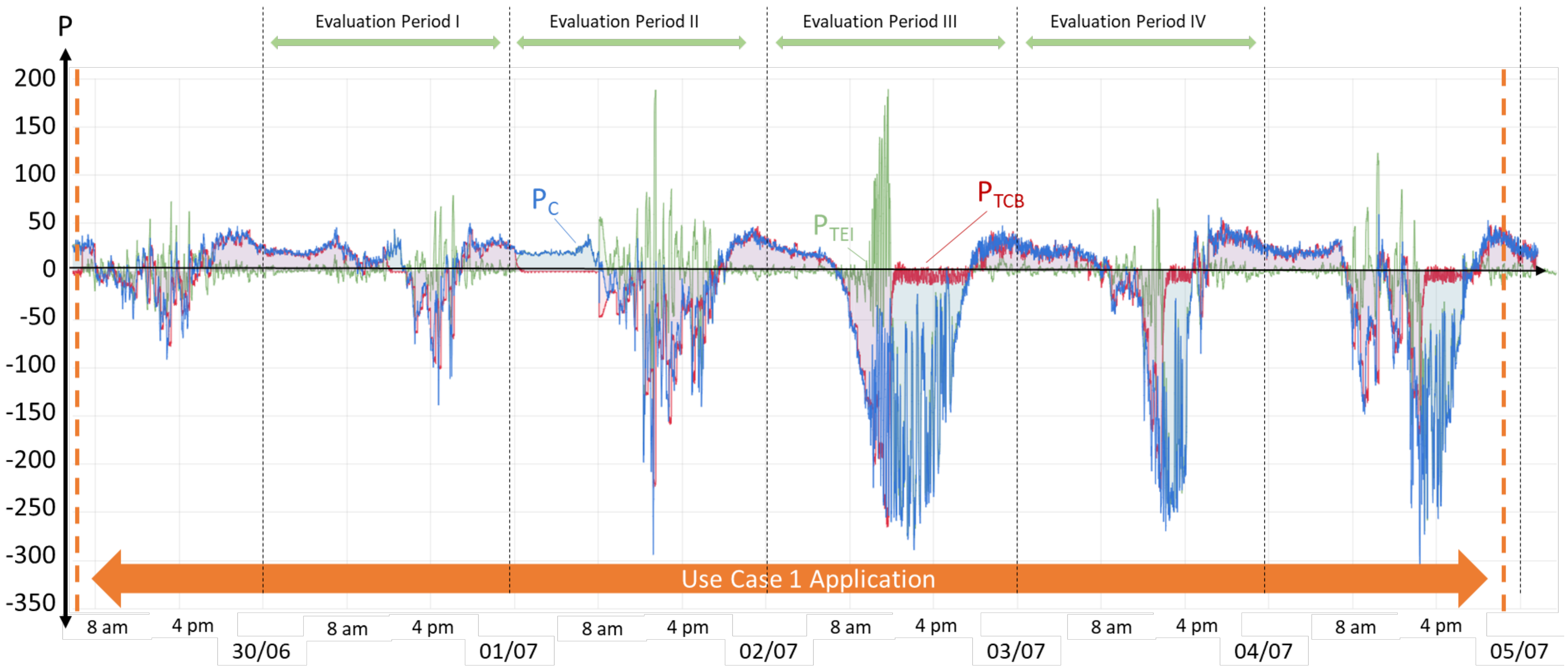

Figure 15: $P_{C,TEI}$, P_{TEI} and P_{TCB} during UC 1 Application from 30/06/2021 0.00 a.m. to 05/07/2021 11.59 p.m.

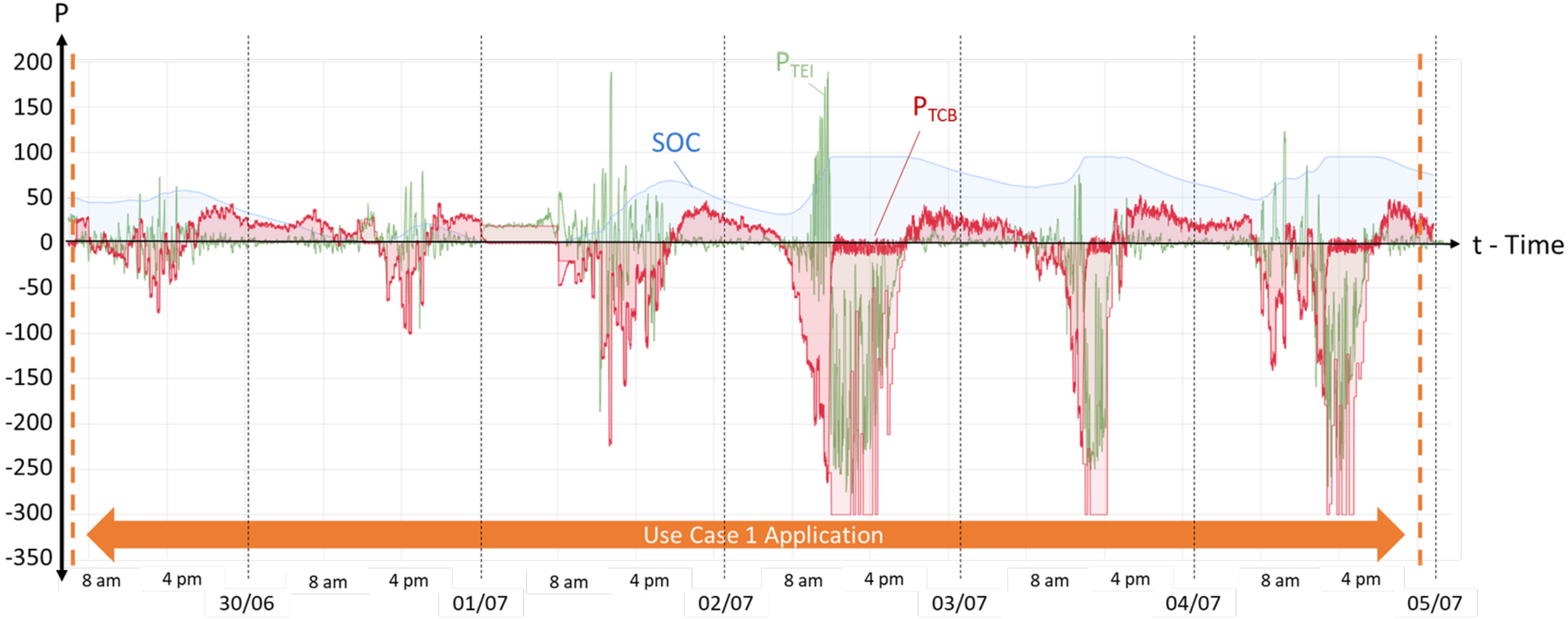

Figure 16: SOC, P_{TEI} and P_{TCB} during UC 1 Application from 30/06/2021 0.00 a.m. to 05/07/2021 11.59 p.m.

7.1 Test 1 – Use Case 1 – 1/7/2021; 0.00 a.m. – 11.59 p.m.

The first evaluation relates to Thursday, July 1st, 2021. The results from Chapter 6 show that the power exchange at the grid connection point is influenced significantly by the local generation from photovoltaics during times with daylight. Therefore, the evaluation for the 24-hour period will be divided into the time period with daylight and dark time. The daylight time of day begins with sunrise at 5.05 a.m. and lasts until 9.53 p.m. The dark time of day lasts from 0.00 a.m. to 5.05 a.m. and 9.53 p.m. to 11:59 p.m.

Weather Data

During the period of investigation rainy and cloud weather prevailed at the beginning of the day until midday. During the daytime the solar radiation increases, due to less cloudiness. Table 4 gives an overview of the relevant weather data and gives an overview of relevant solar radiation data. Figure 17 shows a solar radiation of DIF and GHI over time for the 24 h period. Weather data are procured by a weather data service provider, that provides interpolate data based on closest located weather station.

Table 4: Weather data - 1/7/2021

Indicator	Note	Unit	Max	Min	Average
Temperature		°C	18.8	13.5	15.6
Wind		m/s	5.9	1.7	4.1
Precipitation		mm/m²	0.71		
Solar Radiation	DIF – Diffuse Horizontal Irradiation	W/m²	237.6	0	67.9
	GHI – Global Horizontal Irradiation	W/m²	291.9	0	88.1

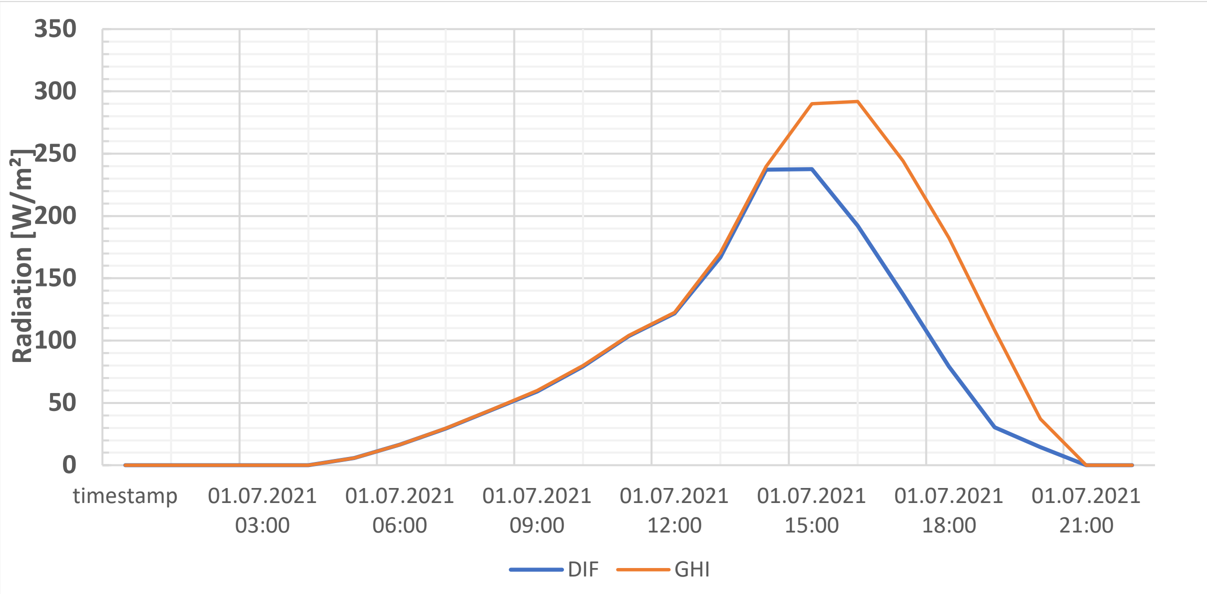

Figure 17: Solar Radiation 1/7/2021 - Abbenhausen (Twistringen)

Measurement Results – Active Power

Figure 18 visualizes the measured power exchange at the network connection point (P_{TEI}) as well as the calculated power exchange that would have occurred, if UC 1 had not been used ($P_{C, TEI}$). Figure 19 visualizes for the entire period the setpoint P'_{TCB} specified by the ALF-C for the storage, the measured input power (P_{TCB}) and the state of charge of the storage SOC_{CBES}.

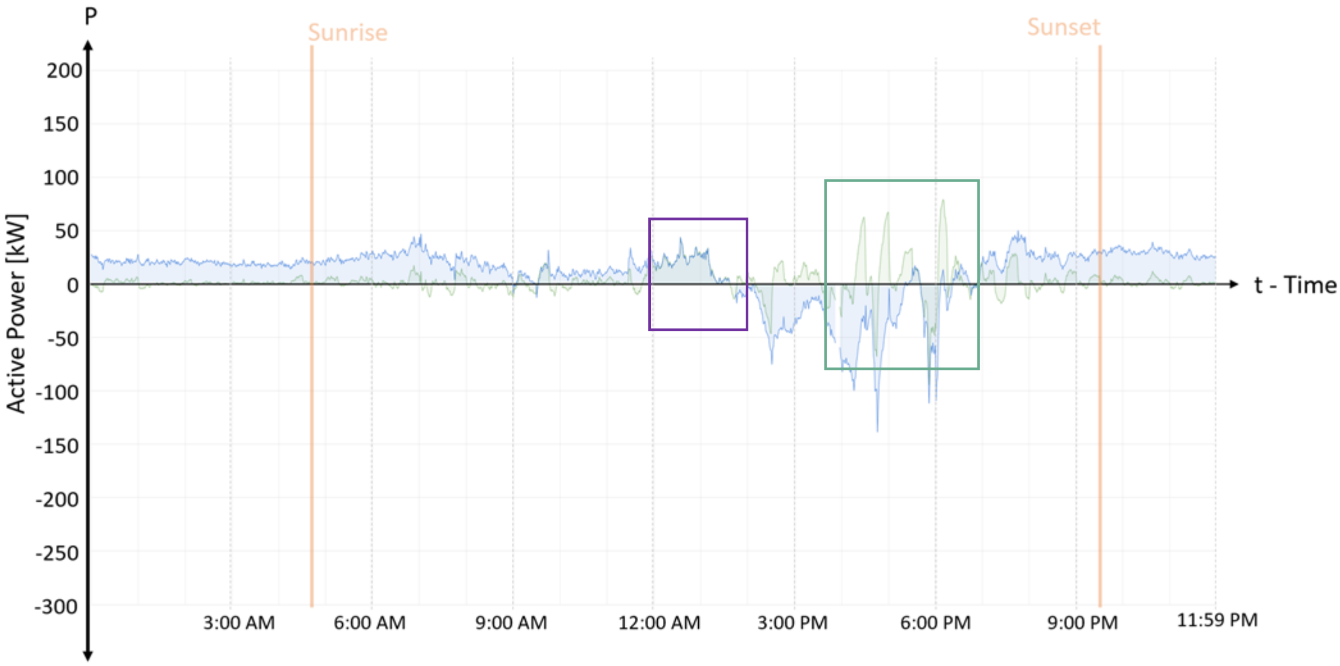

Figure 18: P_{TEI}, $P_{C,TEI}$ - 1/7/2021; 0.00 a.m. - 1/7/2021; 11.59 p.m.

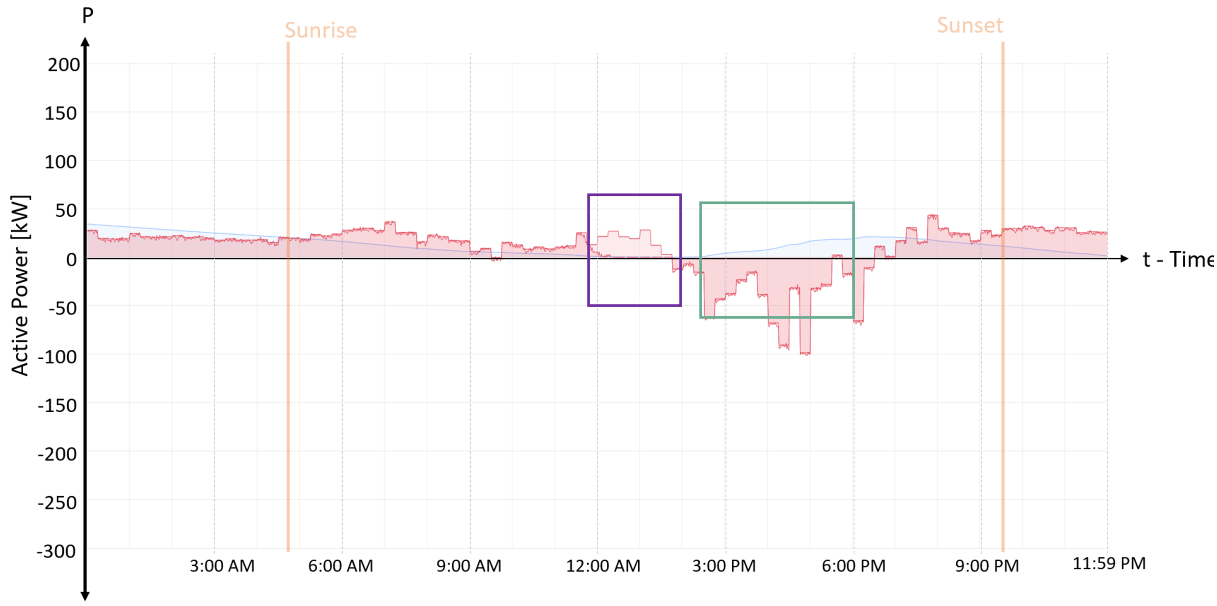

Figure 19: P_{TCB}, P'_{TCB} and SOC_{CBES} - 1/7/2021; 0.00 a.m. - 1/7/2021; 11.59 p.m.

Measurement Results – Energy Data Substation and SOC Battery

Table 5: Relevant Energy Data 1/7/2021; 0.00 a.m. - 1/7/2021; 11.59 p.m.

Indicator	Asset	Start	End	Delta
$E_{TEI,+}$	Substation	150,089 kWh	150,256 kWh	167 kWh
$E_{TEI,-}$	Substation	125,639 kWh	125,571 kWh	68 kWh
SOE_{CBES}*	CBES	301.8 kWh	12.58 kWh	-289.2 kWh
SOC_{CBES}*	CBES	34.3 %	1.43 %	-32.87 %

*SOE (SOC = 100%) = 879,98 kWh

Evaluation - $P_{C,TEI}$

The blue line in Figure 18 indicates the active power exchange if UC would not have been applied. The curves show a power flow from the medium voltage network into the community LV network from 0.00 a.m. until 1.38 p.m. This indicates that the generation of local PV did not generate enough power to meet the community's demand. From 1.42 p.m. to 6.53 the p.m. the local PV generation is higher than local consumption leading to a negative power flow. During this period an import power flow is partially taking place, indicating that generation is decreasing, very likely as result of passing clouds that were covering the sun. During the night, the curve of $P_{C,TEI}$ is exclusively above the zero line (reference). There are no negative values measured. The measured maximum deviation from the zero line is 39.1 kW, the measured minimum deviation from the zero line is 13.5 kW. The average measured deviation is 22.51 kW. During the daytime, the $P_{C,TEI}$ fluctuates with greater deviations from the value 0. The fluctuation becomes greater and the fluctuations faster (gradients). There are high peaks in both positive (reference from the MV network) and negative directions (export to the MV network). The measured maximum deviation from the zero line is 46.8 kW, the measured minimum deviation from the zero line is 0.378 kW. The measured average deviation from the zero line is 18.55 kW.

Evaluation - P_{TEI}

During the night, P_{TEI} fluctuates around the zero line. Both positive and negative values occur. The measured maximum deviation from the zero line is 11.8 kW. The measured average deviation is 2.12 kW. During the daytime, the P_{TEI} fluctuates with greater deviations from the value 0. The fluctuation becomes greater and the fluctuations faster (gradients). There are high peaks in both a positive direction (supply from the MV network) and negative peaks (export into the MV network). The measured maximum deviation.

Table 6 gives an overview of the key results of the measurements from the 1st of July 2021.

Table 6: Overview of Key Measurement Results of P_{TEI}, $P_{C,TEI}$

	Day-Time				Night-Time			
	P_{TEI}	$P_{C,TEI}$	Delta	Delta	P_{TEI}	$P_{C,TEI}$	Delta	Delta
	[kW]	[kW]	[kW]	[%]	[kW]	[kW]	[kW]	[%]
Max	94	139	-45	-32,4	11,8	39,1	-27,3	-70
Min	0	0,044	-0,044	-	0	13,5	-13,5	
Average	10,59	24,54	-13,95	-57	2,12	22,51	-20,4	-91

All in all the results shown in Figure 18 as well as Table 6 show that the graph of P_{TEI} most of the time is closer located to the zero line than $P_{C,TEI}$, which indicates that the application of UC 1 leads to a reduction of the peak value of P_{TEI}, the average as well as to a reduction of the amount of energy exchanged at the grid connecting point. With the application of UC 1 during night-times the peak value of $P_{C,TEI}$ could be reduced by 45 kw (32,4 %) and the mean value by almost 14 kW (57%). The minimum measured value in both cases is almost zero.

Inertia of 15-Minutes Measurement-Control-Cycle

However, the applied measurement-control cycle with a repetition interval of 15 minutes does not manage to maintain P_{TEI} exactly zero. The reason is that an adjustment of the consumptions or discharge of the CBES is triggered every 15 minutes and maintained constant for that period. During this period, the community's power demand and/or PV feed-in increases or decreases. The 15 minutes inertia/delay of the adjustment of the battery (or flexible loads on a later stage of implementation) leads to power fluctuation.

Lack of Flexibility Availability - CBES SOC 100% reached (Purple Brackets in Figure 19)

At the 11.49 a.m. the CBES is close to being fully discharge SOC = 0 %. As result of a CBES safety function the CBES EMS begins to slowly decrease the discharging power until 12.22 p.m. at which P_{TCB} = 0 and SOC_{CBES} = 0 %. As result P_{TEI} equals $P_{C,\,TEI}$ from 12.32 a.m. to 1.45 p.m. From 1.45 p.m. the battery begins to charge, since a positive value of P_{TEI} (export power) is measured at the MV/LV grid connecting point.

Demand Peaks as result of Measurement-Control-Cycle Inertia.

The green marked area of Figure 18 is highlighted in Figure 20 and Figure 21. Figure 20 illustrates that during the daytime the UC 1 application produces a fluctuating power flow (P_{TEI}) with significant power exchange peaks. 3 consumption peaks were measured with 62.4 kW, 66.6 kW and 79 kW. Also negative peaks were measured with a value of -68 kW and - 94 kW.

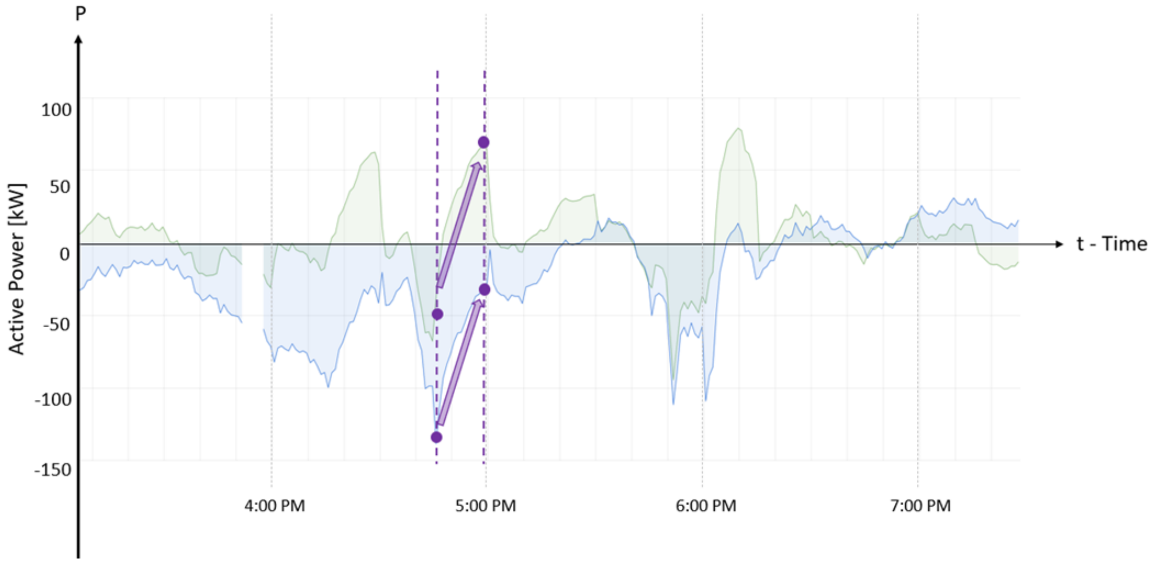

Figure 20: Test 1 - Caused Demand Peaks - P_{TEI} and $P_{C,\,TEI}$

These high peak values are the result of the fluctuating generation from the PV systems and the 15-minute inertia of the measurement-control-cycle. The delayed adjustment of the load of the CBES (charging or discharging) can lead to larger import or export power flows at the grid connection point in case generators increase generation or decrease consumption. Figure 20 and Figure 21 show an example in which:

1.) The ALF-C receives the measurement value P_{TEI} = -68 kW

2.) The ALF-C triggers the CBES to increase consumption by 68 kW up to the value of P_{TCB} = 101 kW.

3.) The CBES maintains 101 kW active power of consumption for 15 minutes. Meanwhile the power flow at the grid connection point decreases by 135,3 kW (blue curve) as result of a reduction of PV infeed. This leads to an increase of P_{TEI} (green curve) by 135,3 kW reaching a value of 67 kW.

4.) The ALF-C receives an updated measurement value P_{TEI} = 67,3 kW.

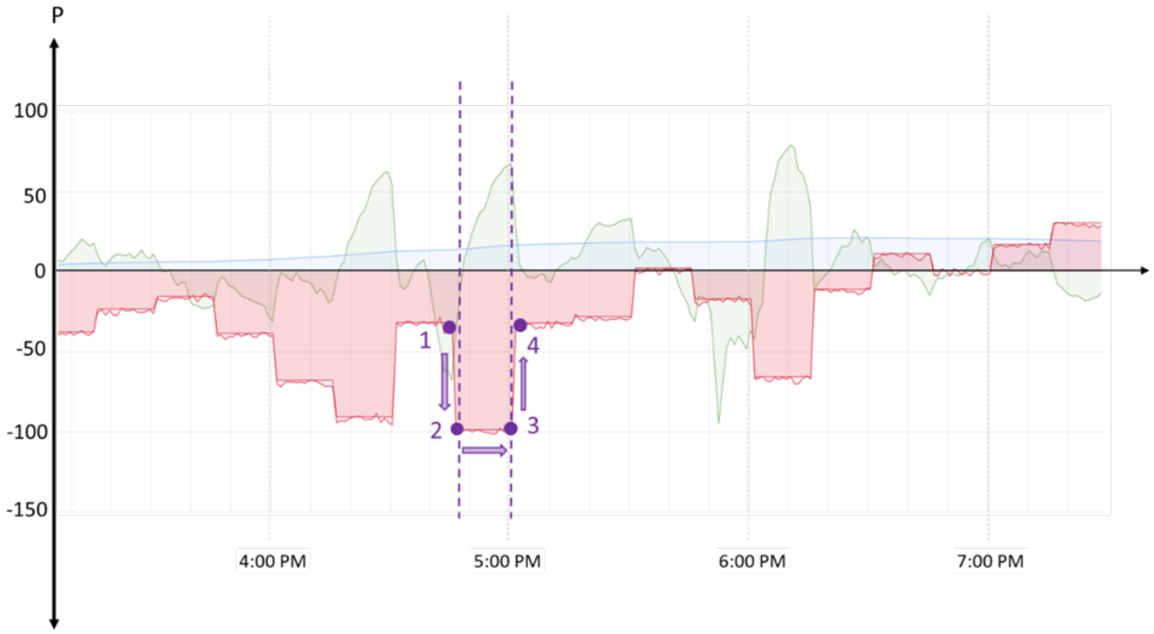

Figure 21: Test 1 - Caused Demand Peaks - P_{TCB}

Conclusion / Lessons Learned – Test 1 - Use Case 1 – 1/7/2021; 0:00 a.m. –11:59 p.m.

- The power demand of communities during night-times is lower and more evenly compared to day times
- During daytimes the power demand/power export is fluctuating with high gradients as of renewable generation from PV systems.
- The PV power generation is fluctuating with high gradients due to the close location of the generators and the high sensitivity to the solar radiation from the sun.
- The battery storage does not have sufficient storage capacity to completely compensate for the imbalance between energy generation and consumption.
- A local balancing mechanism based on a soft real time measurement control cycle (15-minutes) is not able fully compensate all peaks and reach a value of P_{TEI} = 0 kW at the grid connection point.
- The fluctuating infeed from PV generators in conjunction with the inertia of a soft real time local balancing mechanism can lead to positive power exchange peaks (demand peaks) at the grid connection point, which would not have occurred without UC 1 balancing.
- The application of the UC 1 local balancing mechanisms during night times reduced power exchange peaks by 23.1 kW (50%) and the average demand peaks by 9.1 kW (38%).
- The application of the UC 1 local balancing mechanisms during day times reduced power exchange peaks by 106 kW (36%) and the average consumption by 15 kW (37%).
- Weather forecasts do not provide the required quality to forecast generation fluctuations from PV-generators.

7.2 Test 2 – Use Case 1 – 2/7/2021; 0.00 a.m. – 11.59 p.m.

Test two takes place on Friday, the 2nd of July 2021. The daylight time of day begins with sunrise at 5.06 a.m. and lasts until 9.53 p.m. The dark time of day lasts from 0.00 a.m. to 5.06 a.m. and 9.53 p.m. to 11.59 p.m.

Weather Data

Friday, the 2nd of July 2021 was a mixed summer day. The temperature values in Table 7 indicate a rather cold summer day with moderate wind. The values in Table 5 as well as the solar radiation curve in Figure 22 indicate sunshine through the day.

Table 7: Weather Data - 2/7/2021 for Abbenhausen (Twistringen)

Indicator	Note	Unit	Max	Min	Average
Temperature		°C	19.8	14.1	16.9
Wind		m/s	5.0	1.8	3.4
Precipitation		mm/m²	0		
Solar Radiation	DIF – Diffuse Horizontal Irradiation	W/m²	176.2	0	73.6
	GHI – Global Horizontal Irradiation	W/m²	610.9	0	238.1

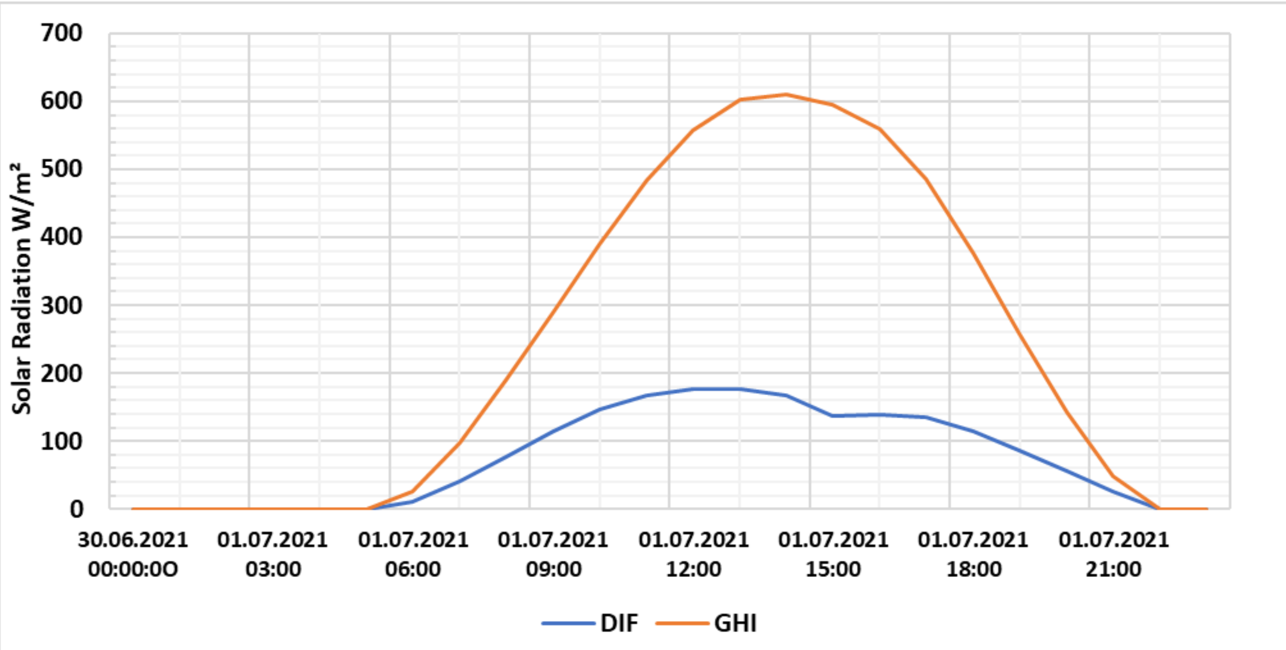

Figure 22: Solar Radiation - Abbenhausen - 2/7/2021 - 0.00 a.m. to 11.59 p.m.

Measurement Results – Power Exchange at Substation

Figure 23 visualizes a fluctuating P_{TEI} and $P_{C, TEI}$. Figure 23 visualizes for the entire period the setpoint P'_{TCB} specified by the ALF-C for the storage, the measured input power (P_{TCB}) and the state of charge of the storage SOC_{CBES}.

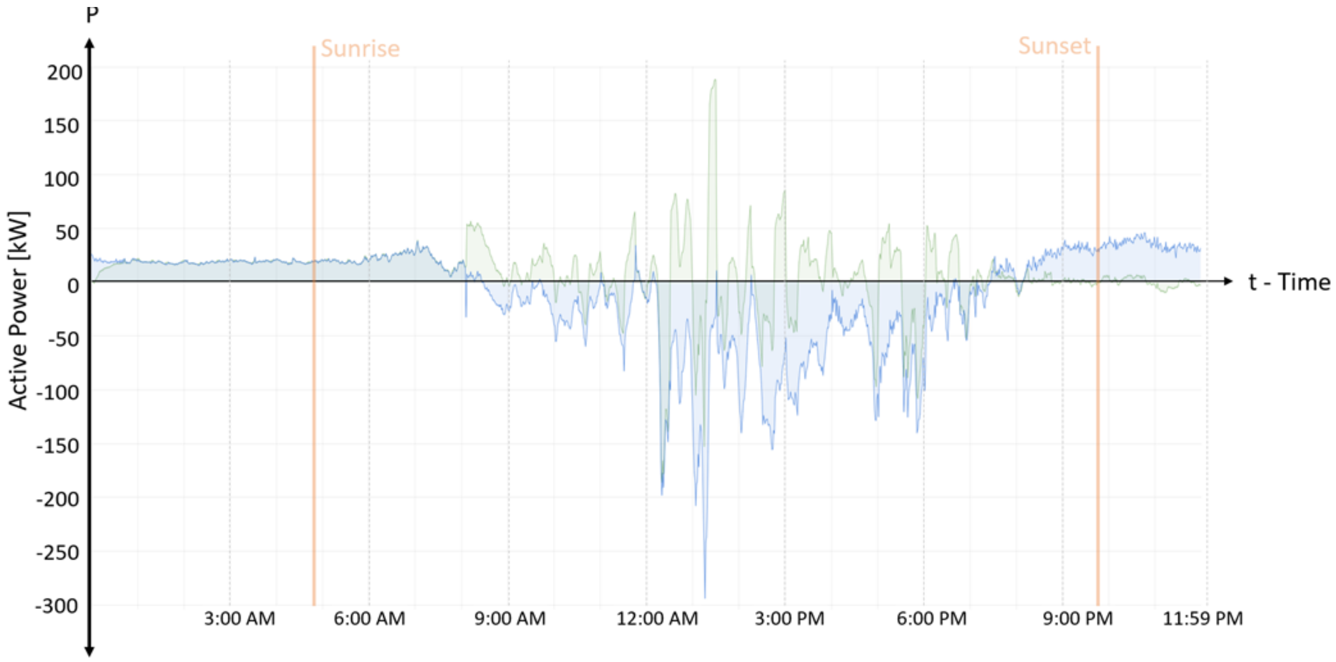

Figure 23: P_{TEI}, $P_{C, TEI}$ - 2/7/2021; 0:00 a.m. - 11.59 p.m.

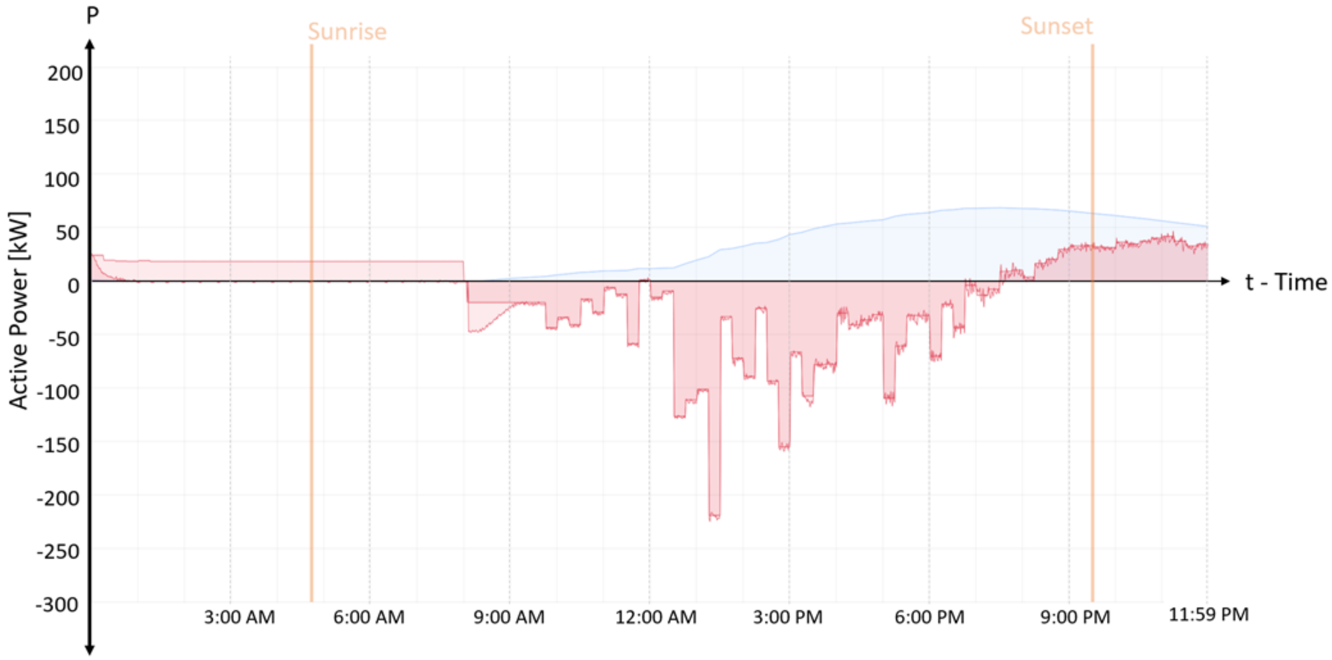

Figure 24: P_{TCB}, P'_{TCB} and SOC_{CBES} - 2/7/2021; 0:00 a.m. - 11:59 p.m.

0.00 a.m. – Beginning of the Day: The day begins with an almost discharged CBES (SOE = 12.3 kWh; SOC = 1.4%). The energy community would have had a demand of $P_{C,TEI}$ = 25.6 kW, however UC 1 lead to a reduction to P_{TCB} = 1.16 kW through the use of the storage system.

0.04 a.m. – 7.58 a.m. - CBES reaches SOC = 0%: The CBES reaches its minimum SOC. Therefore the P_{TCB} begins to increase and until it equals $P_{C,TCB}$ of about 19 kW. Meanwhile the ALF-C continues to trigger the CBES to charge in order to reduce the power exchange P_{TCB}.

8.05 a.m. – 8.09 p.m. - Fluctuating Surplus Generation: At 8.05 a.m. a short term export peak of P_{TEI} = -33 kW leads the ALF-C to trigger the CBES to charge. From this moment on the UC 1 can be applied effective. Due to the short-term reduction of the feed-in power $P_{C,TEI}$ from -33kW to 7.44 kW, the 15-

minute inertia of the measurement control process results in a consumption peak P_{TEI} = 53.9 kW and this remains almost constant for 15 minutes. Until 8.09 p.m. the fluctuations of $P_{C,TEI}$ and P_{TEI} point out that the generation in the network must have fluctuated strongly, presumably due to passing clouds, although the solar radiation data in Figure 22. The example shows that the available weather data are not sufficient of quality to reflect shadow that lead to high frequent generation power drop with high gradients. From this point it can be deduced that a weather forecast will probably also not be able to forecast the high-frequency generation fluctuations with large gradients.

8.09 p.m. – 11.59 p.m. - CBES Compensation of Import Power Exchanges: After the point of time at which the community consumes more power than it is generating the CBES covers the open demand. The CBES is charged sufficiently to provide enough energy until the end of the day.

Measurement Results – Energy Data Substation and SOC Battery 2/7/2021; 0:00 – 2/7/2021; 23:59

Table 8 gives an overview of the status of the battery at the beginning and the end of the 2nd of June 2021.

Table 8: Imported and Exported Energy and CBES SOE/SOC - 2/7/2021

Indicator	Asset	Start	End	Delta
$E_{TEI,+}$	Substation	150,256 kWh	150,633 kWh	377 kWh
$E_{TEI,-}$	Substation	125,732 kWh	125,906 kWh	173 kWh
SOE_{CBES}*	CBES	12.3 kWh	439.9 kWh	+427.5 kWh
SOC_{CBES}*	CBES	1.4 %	51 %	+49.6 %

*SOE (SOC = 100%) = 879,98 kWh

Table 9 compares the values of the power exchange at the grid connection point with and without the application of UC 1 for day and night-time. The result points out at for both times of the day the peak power and average power exchange could be reduced. However, due to the fact the battery already reached its limit at 11.40 a.m. The necessary flexibility wasn't available to compensate the power peaks caused by PV-generators during the midday.

Table 9: Comparison of Power Exchange with and without application of UC 1

	Day-Time				Night-Time			
	P_{TEI}	$P_{C,TEI}$	Delta	Delta	P_{TEI}	$P_{C,TEI}$	Delta	Delta
	[kW]	[kW]	[kW]	[%]	[kW]	[kW]	[kW]	[%]
Max	188	294	-106	-36	22.9	46	-23.1	-50
Min	0	0	-0,044	-	0.06	15.6	-15.5	-99.3
Average	25.65	40.71	-15	-37	13.81	23.7	-9.1	-38

Conclusion / Lessons Learned

- The battery storage does not have sufficient storage capacity to completely compensate for the imbalance between energy generation and consumption.

- A local balancing mechanism based on a soft real time measurement control cycle (15-minutes) is not able fully compensate all peaks and reach a value of P_{TEI} = 0 kW at the grid connection point.
- The fluctuating infeed from PV generators and the inertia of a soft real time local balancing mechanism leads to power demand peaks at the gird connection, that would not have occurred without UC 1 balancing.
- The application of the UC 1 local balancing mechanisms during night times reduced power exchange peaks by 23.1 kW (50%) and the average demand peaks by 9.1 kW (38%).
- The application of the UC 1 local balancing mechanisms during day times reduced power exchange peaks by 106 kW (36%) and the average consumption by 15 kW (37%).
- Weather forecast do not provide required quality to forecast generation fluctuations from PV generators.

7.3 Test 3 – Use Case 1 – 3/7/2021; 0:00 a.m. – 11:59 p.m.

Test number three focuses on Saturday, the 3rd of July 2021. The daylight time of day begins with sunrise at 5.07 a.m. and lasts until 9.52 p.m. The dark time of day lasts from 0.00 a.m. to 5.07 a.m. and 9.52 p.m. to 11.59 p.m.

Weather Data

Saturday, the 3rd of July 2021 was a mixed summer day. The temperature values in Table 10 indicate a moderate warm summer day with minor wind. The values in Table 10 as well as the solar radiation curve in Figure 25 indicate more intense radiation throughout the day compared to test day 1 and 2.

Table 10: Weather Data - 3/7/2021 for Abbenhausen (Twistringen)

Indicator	Note	Unit	Max	Min	Average
Temperature		°C	22.6	11.9	17.4
Wind		m/s	2.7	0.2	1.7
Precipitation		mm/m^2	0		
Solar Radiation	DIF – Diffuse Horizontal Irradiation	W/m^2	261.8	0	112
	GHI – Global Horizontal Irradiation	W/m^2	818.5	0	318.8

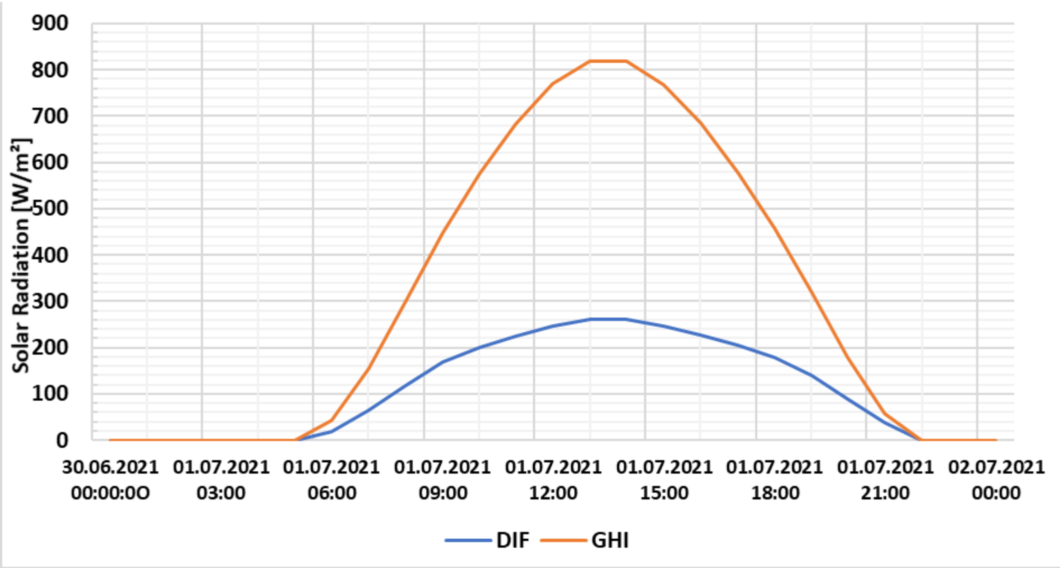

Figure 25: Solar Radiation - Abbenhausen - 3/7/2021 - 0:00 a.m. - 11:59 p.m.

Measurement Results – Power Exchange at Substation

Figure 26 visualizes a fluctuating P_{TEI} and $P_{C,\ TEI}$. Figure 27 visualizes for the entire period the setpoint P'_{TCB} specified by the ALF-C for the storage, the measured input power (P_{TCB}) and the state of charge of the storage SOC_{CBES}.

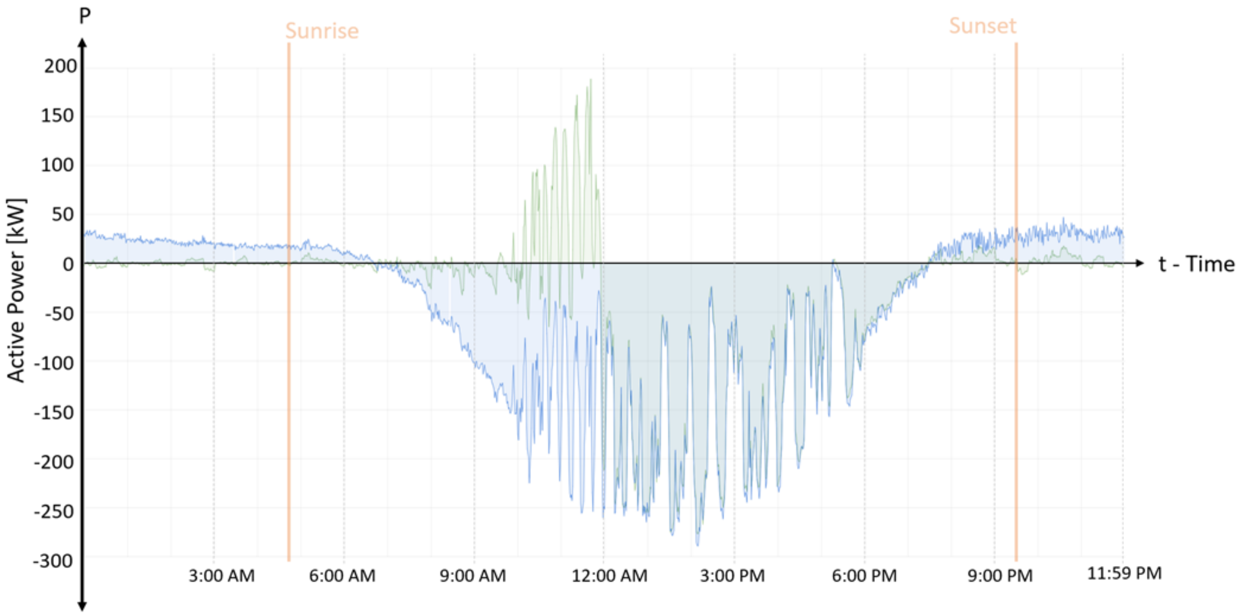

Figure 26: P_{TEI} and $P_{C,\ TEI}$ - 3/7/2021; 0:00 a.m. - 11:59 p.m.

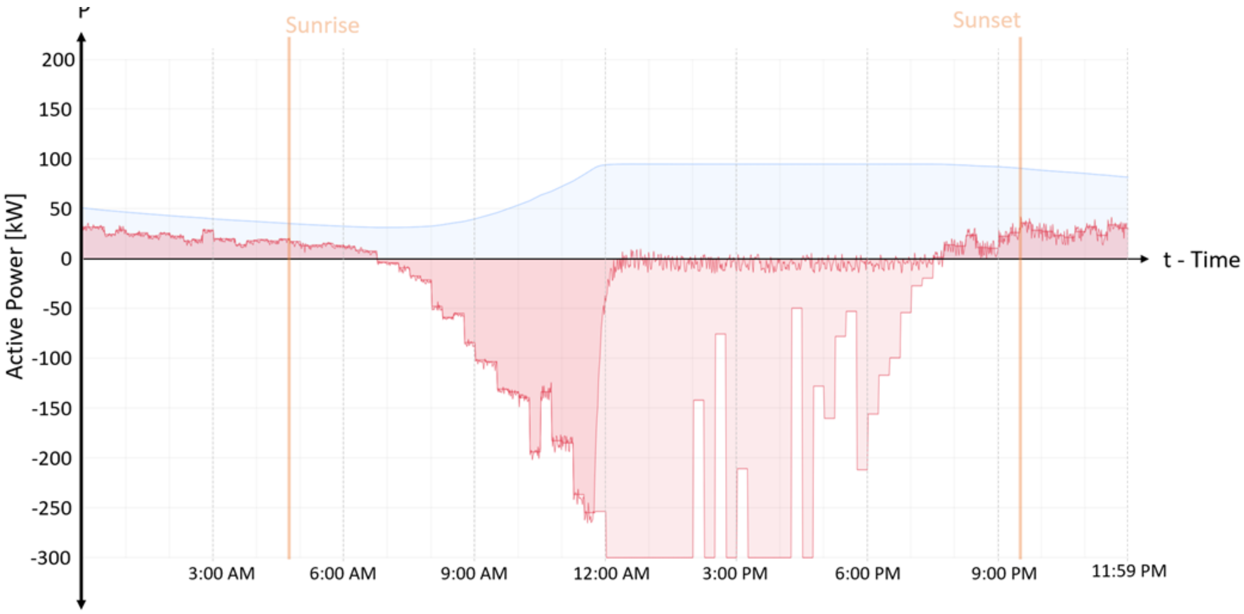

Figure 27: P_{TCB}, P'_{TCB} and SOC_{CBES} - 3/7/2021; 0:00 a.m. - 11:59 p.m.

0.00 a.m. – Beginning of the Day: The day begins with a CBES charging level of 50% (SOE = 12.3 kWh; SOC = 1.4%). The community would have had a demand of $P_{C,TEI}$ = 30.0 kW, however UC 1 leads to a reduction to P_{TCB} = -2.4 kW.

0.00 a.m. – 6.45 a.m. – CBES Compensation of Community Power Exchange: The community load/energy demand is served by the CBES. Small imbalances are compensated for at the grid connection point. P_{TEI} fluctuates between 7.7 kW and -7.9 kW.

6.45 a.m. – 9.51 a.m. – CBES Compensation of Generation Surplus: From 6.45 a.m. on local PV systems begins to generate more energy than demanded by the households. The ALF-C triggers the CBES to switch from discharging to charging mode. In the first half of the period to 11.43 a.m. the ALF-C manages to balance the grid. Due to the continuous increasing feed from PV and due to the 15-minutes-inertia of CBES consumption adaptation, P_{TEI} fluctuates between -7.8 and 32 kW.

9.51 a.m. - 11:43 a.m. - High Power Peaks – Worst Case Scenario: – In this period the worst-case scenario occurs. The UC 1 application lead to very high fluctuation of P_{TEI} with high negative power exchange peaks. P_{TEI} fluctuated between -58 kW and 189 kW. The positive power exchange peaks indicate that the CBES has been charged with energy provided from the medium-voltage network. During this period, the UC 1 mechanism did not contribute to increase self-consumption of the community. This effect is the result of the combination of the 15-minutes-inertia of CBES consumption adaptation and high generation fluctuations from PV systems, as described with Figure 26 and Figure 27.

11.43 a.m. – 0.29 p.m. - CBES reaches SOC Max: At 11.43 a.m. the CBES reaches the critical SOC at which the CBES internal Battery EMS continuously reduces the charging power. At 0.29 p.m. the battery stops charging SOC = 100 % is reached.

0.29 p.m. – 7.30 p.m. – Export of Generation Surplus: In this period local PV generator feed more energy into the grid than demand. Since the CBES is fully charged and not available for balancing, the surplus of power is exported into the MV-network. Therefore, P_{TEI} equals $P_{C,TEI}$, which fluctuates between 276 and – 4.5 kW.

7.19 p.m. – 11.59 p.m. – CBES Compensation of Power Exchange Peaks: At 7.19 p.m. the community start consuming more energy than it is generated by local PV. The CBES starts to discharge to covers the open demand. The CBES is charged sufficiently to provide enough energy until the end of the day. P_{TEI} is fluctuating between the peak value 17.8 and – 11 kW, whereas $P_{C,TEI}$ indicates peak values up to 47.3 kW, in case UC 1 would not have been applied.

Measurement Results – Energy Data Substation and SOC Battery 3/7/2021; 0:00 a.m. – 11:59 p.m.

Table 11 gives an overview of the status of energy that has been imported into the community up to the beginning of the day (0.00 a.m.) and the end of the day. Data are provided by the PLMulti II. The table also provides the SOE and SOC of the CBES at the beginning and the end of the day.

Table 11: Imported and Exported Energy and CBES SOE/SOC - 3/7/2021

Indicator	Asset	Start	End	Delta
$E_{TEI,+}$	Substation	150,633 kWh	150,812 kWh	179 kWh
$E_{TEI,-}$	Substation	143,154 kWh	143,227 kWh	73 kWh
SOE_{CBES}*	CBES	448.8 kWh	719.8 kWh	+271.3 kWh
SOC_{CBES}*	CBES	51 %	81.8 %	+49.6 %

*SOE (SOC = 100%) = 879,98 kWh

Table 12 compares the values of the power exchange at the grid connection point with and without the application of UC 1 for day and night-time. The result points out that for both times of the day the average power exchange could be reduced (night-time by 87%, day-time by 27.7%). However, due to the fact that the battery already reached its limit at 11.40 a.m., the necessary flexibility wasn't available to compensate the power exchange peaks caused by PV generators during the midday.

Table 12: Comparison of Power Exchange with and without application of UC 1

	Day-Time				Night-Time			
	P_{TEI}	$P_{C,TEI}$	Delta	Delta	P_{TEI}	$P_{C,TEI}$	Delta	Delta
	[kW]	[kW]	[kW]	[%]	[kW]	[kW]	[kW]	[%]
Max	277	289	-12	-4.2	17.8	47	29.2	-61
Min	0	0	0	n.a.	0	13	13	-100
Average	65,4	90	-24.6	-27.3	3.11	24.4	21.3	-87

Conclusions

- The battery storage does not have sufficient storage capacity to completely compensate for the imbalance between energy generation and consumption.
- In case local CBES or loads do not provide sufficient capacity to compensate all imbalances during one day, the available flex should be activated at times with highest power exchange peaks in order to make maximize the minimization of P_{TEI}.
- A local balancing mechanism based on a soft real-time measurement control cycle (15-minutes) is not able fully compensate all peaks and reach a value of P_{TEI} = 0 kW at the grid connection point.
- The fluctuating infeed from PV generators and the inertia of a soft real-time local balancing mechanism leads to power demand peaks at the gird connection, that would not have not occurred without UC 1 balancing.
- The application of the UC 1 local balancing mechanisms during night times reduced load exchange peaks by 23.1 kW (50%) and the average demand peaks by 9.1 kW (38%).
- The application of the UC 1 local balancing mechanisms during day times reduced load exchange peaks by 106 kW (36%) and the average consumption by 15 kW (37%).
- Weather forecasts do not provide required quality to forecast generation fluctuations from PV-generators.

7.4 Test 4 – Use Case 1 – 4/7/2021; 0:00 a.m. – 11:59 p.m.

Test number four focuses on Sunday, the 4th of July 2021. The daylight time of this day begins with sunrise at 5.07 a.m. and lasts until 9.52 p.m. The dark time of day lasts from 0.00 a.m. to 5.07 a.m. and 9.52 p.m. to 11.59 p.m.

Weather Data

Sunday, the 4th of July 2021 was a mixed summer day. The temperature values in Table 13 indicate a warm summer day with wind and minor precipitation. The solar radiation curves of this test day show the lowest diffuse horizontal irradiation value and a medium global horizontal irradiation value of all test days.

Table 13: Weather Data - 4/7/2021 for Abbenhausen (Twistringen)

Indicator	Note	Unit	Max	Min	Average
Temperature		°C	23.3	14.5	18.9
Wind		m/s	4.1	0	1.8
Precipitation		mm/m^2	2.6	0	0.4
Solar Radiation	DIF – Diffuse Horizontal Irradiation	W/m^2	234.1	0	94.6
	GHI – Global Horizontal Irradiation	W/m^2	542	0	188.8

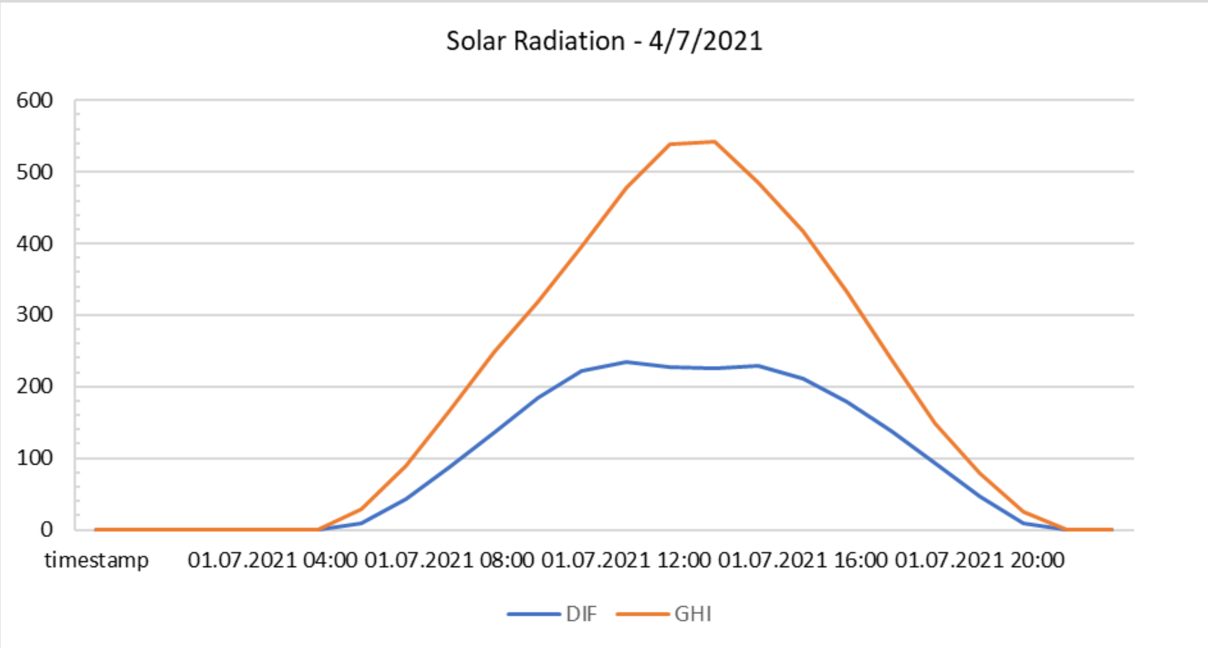

Figure 28: Solar Radiation - Abbenhausen - 4/7/2021 - 0:00 a.m. to 11:59 p.m.

Measurement Results – Power Exchange at Substation

Figure 29 visualizes a fluctuating P_{TEI} and $P_{C, TEI}$ and the setpoint P'_{TCB} specified by the ALF-C for the storage, the measured input power (P_{TCB}) and the SOC of the storage (SOC_{CBES}) for the entire period.

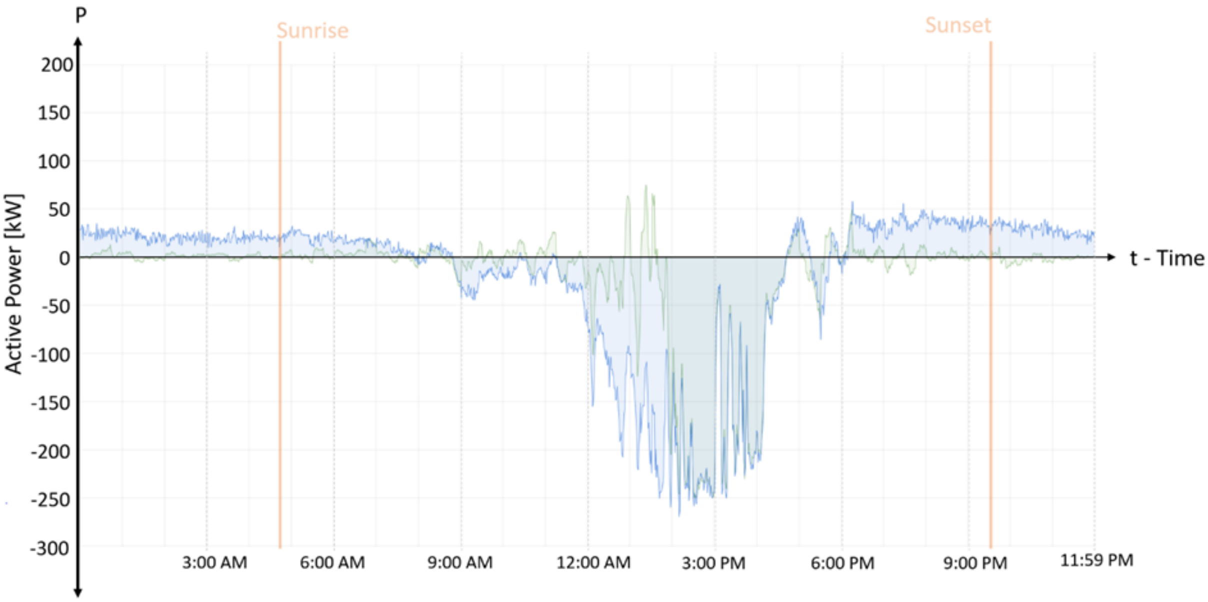

Figure 29: P_{TEI} and $P_{C,\,TEI}$ - 4/7/2021; 0:00 a.m. - 11:59 p.m.

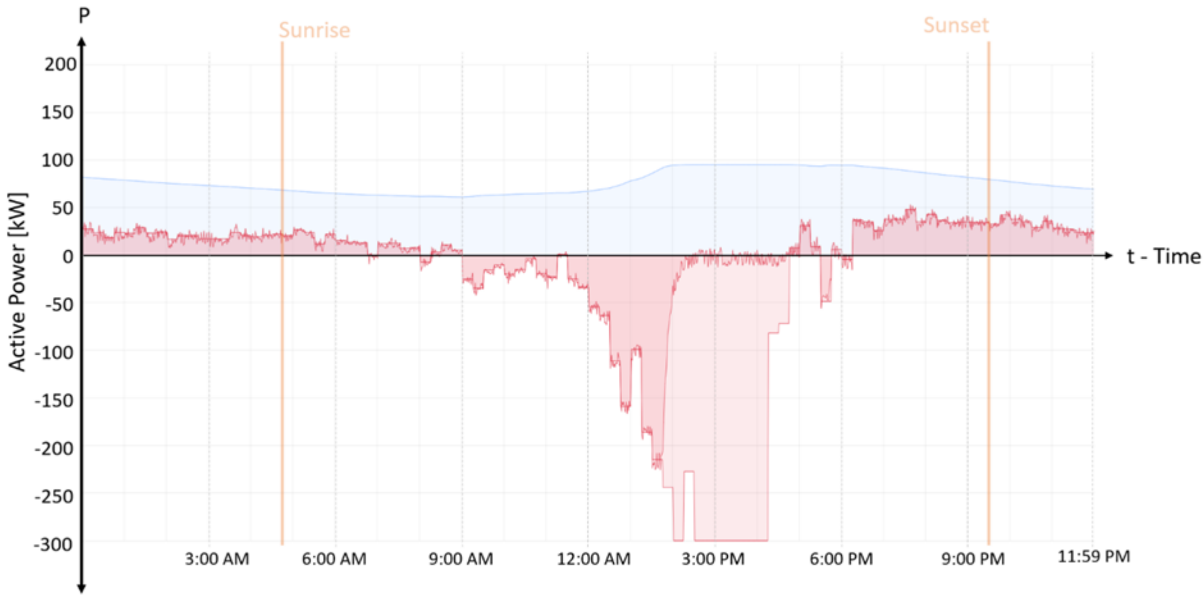

Figure 30: P_{TCB}, P'_{TCB} and SOC_{CBES} - 4/7/2021; 0:00 a.m. - 11:59 p.m.

0.00 a.m. – Beginning of the Day: The day begins with a CBES charging level of 81% (SOE = 448,78 kWh; SOC = 81,7 %). The community would have had a demand of $P_{C,TEI}$ = 28.4 kW, however UC 1 lead to a reduction to P_{TCB} = -2.4 kW.

0.00 a.m. – 8.00 a.m. – CBES Compensation of Community Power Exchange Peaks: The community power/energy demand is served by the CBES. Small imbalances are compensated for at the grid connection point. P_{TEI} fluctuates between 13.4 kW and -5.3 kW.

8.00 a.m.–11.30 a.m. – CBES Behaviour during small fluctuated Generation Surplus: From 8.00 a.m. the small imbalances become bigger. The local PC systems begin to generate more energy than demanded by the households. The ALF-C triggers the CBES to switch from discharging to charging mode and also charging to discharging mode. The positive values of P_{TEI} in this timeslot indicate that the CBES has also charged from the grid. The negative P_{TEI} shows that the local generated energy fed into the MV grid. This happens because of the time delay of 15 min of the ALF-C between measurement and action in the measurement and control cycle. When clouds pass by and interrupt the PV generation, the calculated setpoint doesn't fit to the actual P_{TEI} value anymore. The fluctuation of P_{TEI} in this timeslot lies between -29 and 24.8 kW.

11.30 a.m. - 13:44 a.m. – CBES during Generation Surplus: In this timeslot the ALF-C triggers the CBES to charge. The generated PV is mostly consumed by the CBES. However, due to the 15 min delay in the measurement and control cycle, negative peaks at 12:07pm (-98kW) and 01:12 pm (-113kW) and positive peaks between 12:52 pm and 01:41 pm (59.8kw-75.1) appear. Negative peaks indicate the feed-in into the MV grid of the generated PV, while positive peaks indicate the consummation of energy from the grid that mainly feeds into the CBES.

01.44 p.m. – 02:29 p.m. - CBES reaches SOC Max: At 01.44 p.m. the CBES reaches the critical SOC at which the CBES internal Battery EMS continuously reduces the charging power. At 2.29 p.m. the battery stops charging, SOC = 100 % is reached. Figure 30 shows the given setpoints for the CBES that were not realised by the CBES.

1.44 p.m. – 04.41 p.m. – Export of Generation Surplus: In this period local PV generator feed more energy into the grid than demand. Since the CBES is partly to fully charged and not available for balancing, the surplus of power is exported into the MV-network. P_{TEI} fluctuates between -20 kW and -245 kW.

4.41 p.m. – 6.05 p.m. – CBES Compensation of Power Exchange Peaks: Between 4.41 pm and 06.05 pm fluctuation between discharging and charging of the CBES can be seen in Figure 30. Also here P_{TEI} fluctuates between 30.8 kW and -55 kW.

6.05 p.m. – 23.59 p.m. – End of the day: From 6.05 pm until the end of the day (11.59pm) the CBES discharges and P_{TEI} fluctuated between -19 kW and 14.4 kW.

Measurement Results – Energy Data Substation and SOC Battery 4/7/2021; 0:00 a.m. – 11:59 p.m.

Table 14 gives an overview of the status of energy that has been imported into the community up to the beginning of the day (0.00 a.m.) and the end of the day. Data are provided by the PLMulti II. The table also provides the SOE and SOC of the CBES at the beginning and end of the day.

Table 14: Imported and Exported Energy and CBES SOE/SOC - 4/7/2021

Indicator	Asset	Start	End	Delta
$E_{TEI,+}$	Substation	150.812 kWh	150.924 kWh	112 kWh
$E_{TEI,-}$	Substation	126.906 kWh	127.475 kWh	569 kWh
SOE_{CBES}*	CBES	718.94 kWh	608.95 kWh	-110 kWh
SOC_{CBES}*	CBES	81.7 %	69.2 %	-12.5 %

*SOE (SOC = 100%) = 879,98 kWh

Table 15 compares the values of the power exchange peaks at the grid connection point with and without the application of UC 1 for day and night-time. The result points out at for both times of the day the average power exchange could be reduced. Necessary flexibility wasn't available to compensate the power exchange peaks caused by PV generators during the midday.

Table 15: Comparison of Power Exchange with and without application of UC 1

	Day-Time				Night-Time			
	P_{TEI}	$P_{C,TEI}$	Delta	Delta	P_{TEI}	$P_{C,TEI}$	Delta	Delta
	[kW]	[kW]	[kW]	[%]	[kW]	[kW]	[kW]	[%]
Max	250	269	-19	7	13.4	40,4	-27	66,8

Min	0	0	0	n.a.	0	10	-10	100
Average	36,1	60,8	-27.7	45,5	2.8	23.4	-20.6	88

7.5 Forecast

At the time of writing this deliverable, the forecast based balancing algorithm was developed but not yet implemented in the ALF-C. The implementation is scheduled for August 2021. Consequently, this balancing mechanism could not be tested in the actual demonstrator in the field-test community. However, a simulation was applied, which gives a first insight into the expected results and lessons learned.

Figure 31 shows for the respective investigated days (1st of July to 4th of July 2021) the forecasted power exchange at the MV-feeder $P_{F,TEI}$, shown as a yellow line titled “Cal_iOS_kW”, and the measured power exchange (P_{TEI}), shown as a blue line titled “Real_iONS_kW”. The forecast of the power exchange peaks at the MV-feeder has been computed based on forecast for generation and a forecast of consumption. The forecast of generation is based on a forecast for PV module generation. This data is provided by a service provider at 0.00 a.m. each day. The power exchange forecast is based on a standard load profile (SLP) that has been scaled up according to the number of households located in the grid.

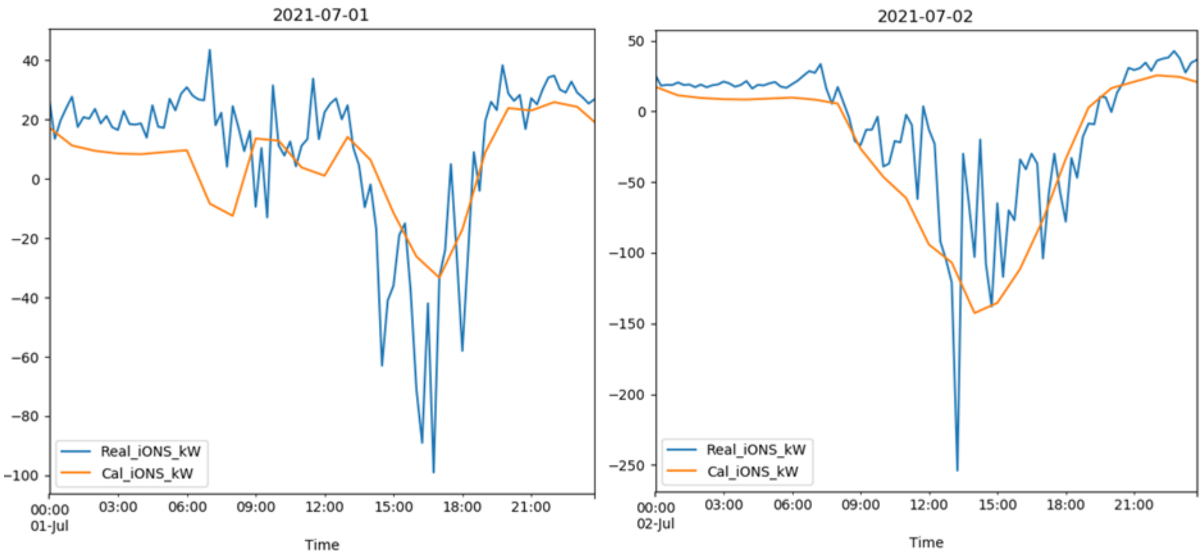

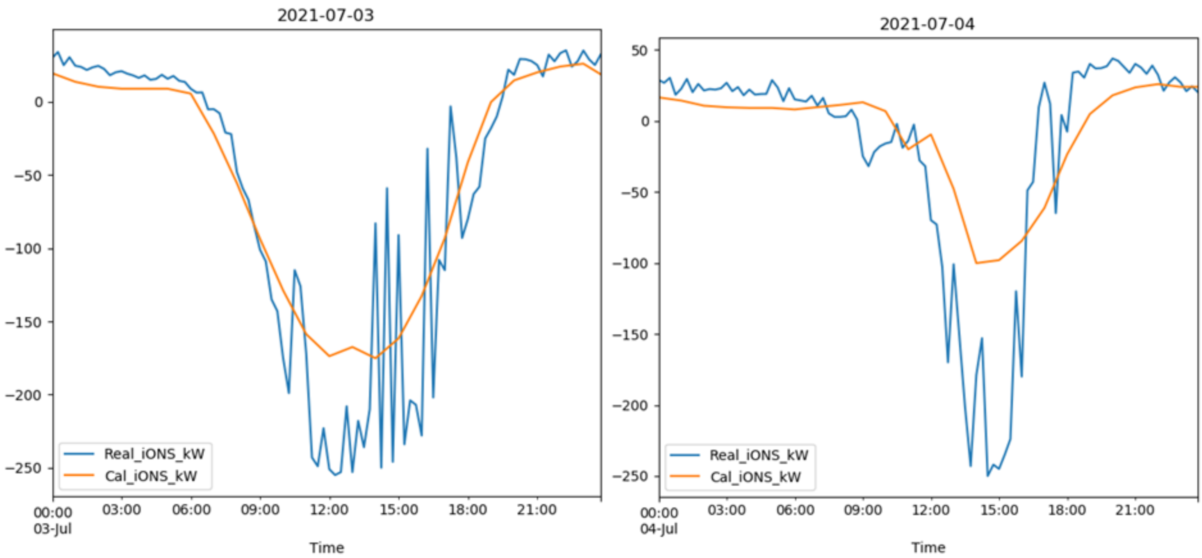

Figure 31: Forecasting of P_{TEI}

The results show that the forecasts of power exchange for each day generally follow the trend of the measured power. Therefore, the forecast gives a good indication of the expected average net power exchange at the grid connection point. However, the resolution of data is not high enough to forecast high frequent fluctuations of PV generation which significantly affects the net power exchange at the substation (P_{TEI}).

Furthermore, the graphs indicate differences between the forecasted power exchange peaks and measured peaks. During the day, differences reach up to 150 kW while at night they are only 8 kW. This might indicate that input data for the forecaster needs to be more accurately scaled.

8 Evaluation based on Project KPIs

Avacon's target is to implement a local balancing mechanism that enables an energy community to become more self-sufficient by reducing the energy and power exchange with the public MV-network at the grid connection point. Therefore, the energy and power exchange at the network connection point shall be minimized. The success of the UC 1 application is assessed based on four KPIs shown in Table 16. The KPIs are determined for the period of July 1st 2021 at 0.00 a.m. to July 4th 2021, 11:59 pm. Deliverable 5.2 provides a detailed description on the methodology of determination and calculation of each KPI. The following sections will describe the results, including interim results as well as a description of the calculation methodology, in case it deviates to the methodology described in D5.2.

Table 16: UC 1 KPI Overview

ID	Name	Description	Unit
KPI_DE_01	Reduction of Energy Exchange at the MV/LV grid connection point	• To improve customers' engagement and facilitate their fair participation to market. • To unlock flexibility to address local congestion and voltage stability issues.	%
KPI_DE_02	Education of power peaks	• To improve customers' engagement and facilitate their fair participation to market. • To unlock flexibility to address local congestion and voltage stability issues.	%
KPI_DE_03	Increase in self-consumption	• To improve customers' engagement and facilitate their fair participation to market. • To unlock flexibility to address local congestion and voltage stability issues.	%
KPI_DE_04	Maximization of Islanding Duration	• To improve customers' engagement and facilitate their fair participation to market. • To unlock flexibility to address local congestion and voltage stability issues.	%

8.1 KPI 1-KPI_DE_01 – Reduction of Energy Exchange at MV Feeder

KPI 1 shall evaluate the relative reduction of energy exchange at the grid connection point for a 2, 6-, 12-, 24-, 48- and 96-hours duration. From the KPI 1 description in D5.2 it could be interpreted that the energy consumption from the medium-voltage network should be evaluated. However, the aim of the KPI is to minimize the entire energy exchange at the grid connection point and to evaluate it with this KPI. The following formula is used so that the result measures the increase or decrease in the energy exchange as a relative value.

Formula for the calculation of KPI 1 – RED:

$$RED = \frac{\sum_{t_0}^{T} |Energy\ Exchange\ no\ Islanding|_t - \sum_{t_0}^{T} |Energy\ Exchange\ Islanding|_t}{\sum_{t_0}^{T} |Energy\ Exchange\ no\ Islanding|_t} * 100$$

$$= \frac{\sum_{t_0}^{T} |E_{C,TEI}|_t - \sum_{t_0}^{T} |E_{TEI}|_t}{\sum_{t_0}^{T} |E_{C,TEI}|_t} * 100$$

Table 17 gives an overview over the measurement results and the determined value of KPI 1.

Table 17: KPI 1 - Measurement Values and KPI Calculation

Date	Time	Duration [t]	$E_{C,TEI}$	E_{TEI}	KPI
[d/m/yyyy]	[CET]	[h]	[kWh]	[kWh]	[%]
1 / 7 / 2021	0.00 am – 01.59 am	2	42.10	4.84	88.51
1 / 7 / 2021	0.00 am – 05.59 am	6	123.78	12.56	89.86
1 / 7 / 2021	0.00 am – 11.59 am	12	229.58	42.14	81.64
1 / 7 / 2021	0.00 am – 11.59 pm	24	429.24	166.05	61.31
1 / 7 / 2021 - 2 / 7 / 2021	0.00 am – 11.59 pm	48	1424.52	722.70	49.27
1 / 7 2021 - 4 / 7 / 2021	0.00 am – 11.59 pm	96	4291.33	2.467.15	42.51

Description of Results:

The values in Table 17 show that the application of UC 1 with the given field test setup enabled the community to reduce the energy exchange at the grid connection point up to 90 % for short periods of UC 1 application and 43 % for long periods of UC 1 application. The results indicate that on a longer duration of application UC 1 the relative amount of energy exchange at the grid connection point decreases. The major reason of this effect is the short sunshine duration on day 1, which leads to a little battery charging and a lack of available energy provided by the CBES. In contrast to that, on days 3 and 4 local generators generate more energy than storage capacity could be provided by the CBES. Consequently, the CBES reached SOC Max at midday and for the rest of the day generated surplus was exported at the grid connecting point.

Implication for future Investigations:

The results shown above do not differentiate between daylight and night-time periods. However, as seen in the measurement values of P_{TEI} and $P_{C,TEI}$, the fluctuating infeed from PV generator in conjunction with the 15-minutes inertia of the measurement-control cycle will lead to energy exports and consequently different values of KPI 1 for day time and night time periods.

Conclusion:

The results show that a local soft real-time balancing mechanism based on a 15-minutes measurement control cycle and with a CBES with 850 kWh of storage capacity is capable to significantly decrease the energy exchange between an MV network an energy community consisting of 89 households and a total installed PV generation capacity of 302 kW. The success of the mechanism is primarily depending on the availability of storage capacity.

8.2 KPI 2 – KPI_DE_02 – Reduction of Power Peaks

KPI 2 evaluates the ability of the ALF-C measurement-control-cycle balancing mechanism to reduce the maximum value of power peak exchange at the grid connection point during the application of UC 1 for a duration of 2-, 6-, 12-, 24-, 48- and 96-hours. The KPI determines the relative reduction or increase of the highest measured peak, when UC 1 has not been applied ($|P|_{C,TEI,\ MAX}$) and the highest peak values, that has been measured, while UC has been applied ($|P|_{TEI,\ MAX}$).

The KPI is determined by applying following formula:

$$Peak\ Reduction = \frac{|P|_{Max,no\ Islanding}(T) - |P|_{Max,with\ Islanding}(T)}{|P|_{Max,no\ Islanding}(dt)} * 100 = \frac{|P|_{C,TEI}(T) - |P|_{TEI}\ (T)}{|P|_{C,TEI}(dt)} * 100$$

Table 18 gives an overview over the measurement results and the determined value of KPI 2.

Table 18: KPI 2 - Measurement Values and KPI Calculation

Date	Time	Duration [t]	$E_{C,TEI}$	E_{TEI}	KPI
[d/m/yyyy]	[CET]	[h]	[kWh]	[kWh]	[%]
1 / 7 / 2021	0.00 am – 02.00 am	2	27.7	7.30	73.65
1 / 7 / 2021	0.00 am – 06.00 am	6	30.9	8.04	73.98
1 / 7 / 2021	0.00 am – 11.59 am	12	46.8	26.20	44.02
1 / 7 / 2021	0.00 am – 11.59 pm	24	139.0	94.00	32.37
1 / 7 / 2021 - 2 / 7 / 2021	0.00 am – 11.59 pm	48	294.0	188.00	36.05
1 / 7 2021 - 4 / 7 / 2021	0.00 am – 11.59 pm	96	294.0	277.00	5.78

Description of Results:

The values in Table 18 show that the application of UC 1 with the given field test setup enables the reduction of power peaks of a community with the MV-network for up to 73 % for short periods of application and 5.8 % for long periods of UC 1 application. The results indicate that for a longer duration of the application of UC 1 the relative amount of reduction decreases significantly. The reason is ones again the lack of availability of the CBES due to the limit of storage capacity. Figure 15 in conjunction with Figure 16 show, that on day 3 (July, the 3rd) and day 4 (July, the 4th) during middays, the high amount of exported power ($P_{C,TEI}$) and energy ($E_{C,TEI}$), as result of the high amount of generated power and energy from local PV, cause the CBES to be fully charge at middays, when $P_{C,TEI}$ are reaching highest peaks. Consequently, the exporting Peaks in the following hour cannot be compensated anymore. So, the lack of ability of the ALF-C to compensate power peaks for long duration of UC 1 application is caused by the lack of flexibility availability.

Implication for future Investigations:

The results shown above do not differentiate between daylight and night-time periods. However, as seen in the measurement values of P_{TEI} and $P_{C,TEI}$, the fluctuating infeed from PV generator in conjunction with the 15-minutes inertia of the measurement-control-cycle will lead to energy exports and consequently different values of KPI 1 for day-time and night-time periods.

Conclusion:

The results show that a local soft real time balancing mechanism based on a 15-minutes measurement control cycle and with a CBES with 850 kWh of storage capacity is capable to significantly decrease the power peaks between the MV network and an energy community, that consists of 89 households and a total installed PV generation capacity of 302 kW. The success of the mechanism is primarily depending on the availability of storage capacity. In order to decrease the total amount of power peaks with the given field test setup, while enabling the community to maximize self-consumption, the strategy of CBES activation (point of time, duration, charging power (P_{TCB}) needs to be improved in such a way that the CBES is still available during middays power peak times. For this purpose, an optimization algorithm is required, that based on a weather forecast determines the optimum point of time to start with charging. The optimization goal has to be the reduction of power peaks while as constraints the CBES has to be fully charged by the point of time at which the local generation is less than local consumption and the CBES has to begin to discharge.

8.3 KPI 3 – KPI_DE_03 – Increase in Self-Consumption

KPI 3 evaluates the ability of the ALF-C measurement-control-cycle balancing mechanism to increase the self-consumption of local generated energy during a 2-, 6-, 12-, 24-, 48- and 96-hour period of UC 1 application. The KPI determines the relative decrease of the amount of energy that has been exported ($E_{TEI,-}$) with the amount that would have been export, if UC 1 would not have been applied ($E_{C,TEI-}$).

The KPI is determined by applying following formula, which is described in detail in Deliverable D5.3:

$$= \frac{\sum_{t=1}^{T}|Energy\ Export\ no\ Islanding|_{i;t} - \sum_{t=1}^{T}|Energy\ Export\ Islanding|_{i;t}}{\sum_{t=1}^{T}|Energy\ Export\ Islanding|_{i;t}} * 100 = \frac{\sum_{t=1}^{T}|E_{C,TEI-}|_{i;t} - \sum_{t=1}^{T}|E_{TEI-}|_{i;t}}{\sum_{t=1}^{T}|E_{TEI-}|_{i;t}} * 100$$

The value of E is determined for each minute by applying following formula on the 1-minute mean values of $P_{C,TEI}$ and P_{TEI}:

$$E = \frac{1}{60} * P$$

Table 19 gives an overview over the measurement results and the determined value of KPI 3.

Table 19: KPI 3 - Measurement Values and KPI Calculation

Date	Time	Duration [t]	$E_{C,TEI}$	E_{TEI}	KPI
[d/m/yyyy]	[CET]	[h]	[kWh]	[kWh]	[%]
1 / 7 / 2021	0.00 am – 02.00 am	2	0	-2.06	n.a.
1 / 7 / 2021	0.00 am – 06.00 am	6	0	-2.59	n.a.
1 / 7 / 2021	0.00 am – 11.59 am	12	-0.55	-14.0	2,434.34

1 / 7 / 2021	0.00 am – 11.59 pm	24	-162.21	-51.20	-68.44
1 / 7 / 2021 - 2 / 7 / 2021	0.00 am – 11.59 pm	48	-725.75	-222.13	-69.39
1 / 7 2021 - 4 / 7 / 2021	0.00 am – 11.59 pm	96	-2,980.11	-1,733.16	-41.84

Description of Results:

The values in Table 19 show that the application of UC 1 leads minor exports of energy during the short term periods, while without the UC application no exports would have been taken place. This effect can be interpreted as the result of the inertia of the 15-minutes measurement control cycle, described in the previous sections. However, in period 3 with a 12-hour application duration an extreme relative increase of 2,434 % (13,45 kWh) has been measured. The high increase is caused by the relative low values of $|E|_{C,TEI-}$. Once again this is the result of the inertia of the 15-minutes measurement control cycle in conjunction with the special situation, that due to the cloudy day, no surplus energy has been generated. Therefore, the results of the first three periods can be interpreted as not be representative. However, the real effect of UC 1 can be evaluated with the last 4 time periods. These periods show the effect, while energy surplus is generated during sunshine hours. The values show that the amount of generated energy surplus can be reduce by up to 70 %. For longer durations the relative amount decreases. This can be interpreted as result of the lack of CBES storage capacity, as described in previous sections and to been seen in Figure 16.

8.4 KPI 4 – KPI_DE_04 – Maximization of Islanding Duration

KPI 4 evaluates the ability of the ALF-C measurement-control-cycle balancing mechanism to increase the duration at which the power exchange at the grid connecting point is less than 10 kW during a 2-, 6-, 12-, 24-, 48- and 96-hour period of UC 1 application. The KPI is determined by applying following formula:

$$\text{KPI4} = \frac{\sum_{t0}^{T} t_{Islanding;\, P_{Breaker} \approx 0}}{\sum_{t0}^{T} t_{No\ Islanding;\, P_{Breaker} \approx 0}} * 100 = \frac{\sum_{t0}^{T} t(|P_{TEI}| \leq 10kW)}{\sum_{t0}^{T} t(|P_{C,TEI}| \leq 10kW)} * 100$$

Table 20 gives an overview over the measurement results and the determined value of KPI 4.

Table 20: KPI 4 - Measurement Values and KPI Calculation

Date	Time	Duration [t]	$E_{C,TEI}$	E_{TEI}	KPI
[d/m/yyyy]	[CET]	[h]	[kWh]	[kWh]	[%]
1 / 7 / 2021	0.00 am – 02.00 am	2	0	2.00	2.00
1 / 7 / 2021	0.00 am – 06.00 am	6	0	6.00	6.00
1 / 7 / 2021	0.00 am – 11.59 am	12	1.40	11.40	10.00
1 / 7 / 2021	0.00 am – 11.59 pm	24	3.13	15.52	12.38

1 / 7 / 2021- 2 / 7 / 2021	0.00 am – 11.59 pm	48	5.58	30.93	25.33
1 / 7 2021 - 4 / 7 / 2021	0.00 am – 11.59 pm	96	9.80	74.80	64.98

Description of Results:

The results shown in Table 20 indicate that, the ALF-C was able to significantly extend the duration for which the community had a net power exchange of less than 10 kW. During the first three time periods, the ALF-C was able to reduce reach P < 10 kW the entire periods For time period 3, 4 and 6 the ALF-C manages to extend the duration up to 70%.

Conclusion:

The results point out that the ALF-C with a local balancing mechanism based on a soft real-time 15-minutes measurement-control-cycle the given field test setup is able to significantly increase the duration of period, at which the power exchange between the community and the feeding grid connection point can be reduced to close to zero (under 10 kW). The temporary uncoupling of the low-voltage network from its MV-feeder was therefore successfully demonstrate. The results have shown that ability of uncoupling primarily depends on the availability of flexibility (CBES storage capacity) and the fluctuating infeed from local PV. High fluctuating gradients of feed-in power from PV leads to high changes of power exchanges, that cannot be compensated by the ALF-C quickly enough, due to the inertia of the 15-minutes measurement-control-cycle. Days with a lot of changes between sunlight and shadows caused by small clouds lead to a reduction of the period for which the community can be uncoupled.

9 Lessons Learned

The field trials focusing on UC1 in WP5 have clearly demonstrated the potential and feasibility of the application of a local balancing mechanism (ALF-C) in LV-grids to enable a community to increase self-consumption of locally generated energy, when practicing energy sharing. Further, the temporary uncoupling from the MV-grid has been successfully tested and has demonstrated the positive effect of a minimization of power peaks and energy exchange at the MV-feeder on the DSO's MV-network. These functionalities form the basis for the upcoming use cases UC 2, UC 3 and UC 4 and can help to improve DSO operations, support the integration of future energy communities and DER.

9.1 Implication on forthcoming Use Case Application and Field Test

The results of UC 1 show that the ALF-C with the given field-test setup is able to temporary minimize the exchange of power and energy as well as temporarily uncouple the LV-grid of the community from the MV-grid. This ability meets the prerequisite for the application of UC 3 and 4, which will be tested at a later stage of this field test. . The knowledge and experience gained in the course of carrying out UC 1 will be taken into account for the continuous development of the ALF-C balancing algorithms. The balancing mechanism can be improved by tuning the current direct-charging approach (measurement-control-cycle) or the addition of alternative approaches, which are described in the following.

Improvement of UC 1 Balancing Approach

The UC 1 results show that high-frequency fluctuations in PV generation in conjunction with the inertia of the 15-minute measurement-control-cycle on a clear summer day can result in a contradictory impact on the target of minimizing the power peaks and energy exchange at the grid connection point.

The balancing mechanisms can be improved by following approaches:

- **Direct-Charging Approach (Measurement-Control-Cycle)**

  This approach lacks from CBES availability during peak times, as shown in previous chapters. Further this approach causes a high-power exchange increase at the point of time, at which the CBES reaches its SOC limit. The approach therefore only has a limited grid friendly and positive system related effect for the DSO. But it has a positive effect on the contribution of maximization of collective self-consumption. However, different approaches might improve the effect during times of CBES availability. For example, the timing of the control cycle can be increased to compensate fluctuation with high gradients, e.g., from 15 minutes to 5 minutes. Alternatively, the limitation of charging and discharging power of local flexibility (e.g. CBES, P_{TCB}), e.g. to 50 % (150 kW), might avoid or reduce positive (consumption) power peak at the substation during day times.

- **Delayed Charging Approach**

  In this approach the battery does not start at the point of time at which local PV-start generate surplus. The start of charging is delayed and begins at a point of time, at which the generation peaks come closer to their maximum. This approach supports the reduction of large power flows as result of high generation peaks. This delay assures that during peak generation, enough storage capacity is available. However, despite the delay it must be assured that the battery is fully charged at the end of the day. The starting point for charging the battery can be determined empirically or based on a forecast of net generation and consumption in conjunction with an optimizer in order to ensure that the CBES is fully charged at the end of the day, in order to make maximum use of available flexibility. This approach supports the maximization of collective self-consumption and reliefs the MV-network.

- **Peak-Shaving Approach**

  The Peak-Shaving approach requires a limit for the maximum value of power exchange at the MV-feeder in relation to the installed PV generation power connected to a single LV grid. Above the set limit, the CBES charges. The activation of the CBES reliefs the MV-grid from additional stress caused by the peaks in generation and increases hosting capacity for additional PV generators or other RES. This approach has a grid-friendly and positive system related effect for the DSO. However, this approach does not contribute to maximize collective self-consumption of energy generated locally.

- **Forecast Based Approach**

  A forecast of generation and demand yields the expected power exchange for the community. Based on the forecast the activation of the CBES can be optimized. As result a setpoint schedule for the CBES is determined. The mechanism enables to minimize the power exchange peaks at the MV-feeder and consequently reliefs the MV-grid from additional stress. Additionally, it enables the maximization of consumption of locally generated energy (collective self-consumption).

9.2 Implication on Future Productive Implementation

The field test has successfully demonstrated that the ALF-C enables a community to practice collective self-consumption of local PV generation by making use of local flexibility.

Figure 21 shows a potential path how UC 1 could be implemented into day-to-day operations. It starts with a large-scaled roll-out of smart secondary substations that provide the necessary data. Additionally, the planned but delayed roll-out of smart meters in Germany could provide additional data about generation and consumption on individual household levels. Thus, the DSO could begin replacing the legacy technologies mentioned in Chs. 3.4 and 3.5 with an ALF-C-enabled smart secondary substation and smart meter with a smart meter control box infrastructure. Once a sufficient number of substations and smart meters has been connected, the migration of DSO owned, private owned battery storage systems and the double-tariff heaters can be started. The next step would be to make active use of the interruption actions for EV-chargers and heat pumps.

The next step, to be demonstrated as part of UC 2, will be to enable the ALF-C to interact with the available flexibility offered by the community CBES and household battery storages to maintain a given setpoint for the power exchange at the grid connection point (P'_{TEI}). This requires the first onboarding of customers after the implementation of additional measurement, control and communication technology.

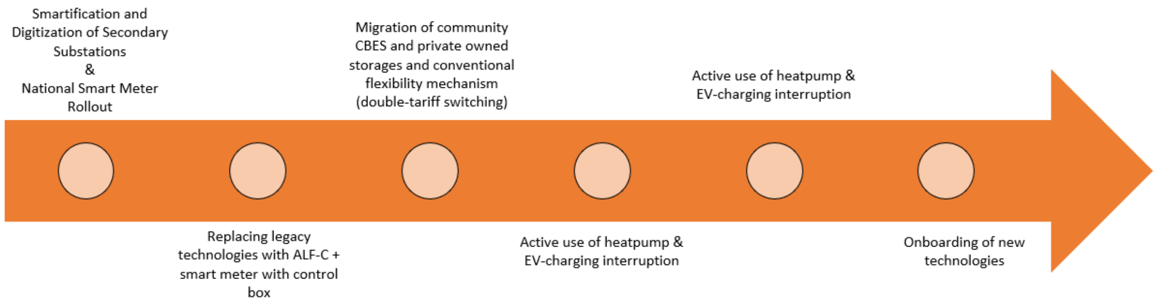

Figure 32: Potential Path of Development for Use Case 1

10 Conclusion

Energy Balance of Local Energy Communities

1.) The community of Abbenhausen with its large penetration of PV modules proved to be a model region for future Local Energy Communities (LEC).

2.) From February 2021 onwards the community produced more energy than it required on most days. The maximum ratio of energy export to import was about eight. The amount of energy surplus often exceeds the capacity of the currently installed battery storage by large margins. This demonstrates that smart energy management systems are required to subsequently utilise the surplus energy economically.

3.) The largest energy generation is realised on clear and sunny days. The challenge on such days is that the surplus energy often exceeds storage capacity. Thus, algorithms that determine when to charge, e.g. peak generation at noon, are essential.

4.) On partly cloudy days a large energy surplus is possible. However, unsteady cloud cover produces steep gradients in generation which need to be managed.

5.) Very low energy generation was realised on overcast days without direct solar radiation. This presents a trade-off between storing energy in the preceding days or simply importing energy from the MV-grid.

Weather Data & Forecasts

6.) Meteorological models do not have sufficient temporal and spatial resolution for an accurate prediction of local solar radiation, i.e. cloud cover, especially partly clouded days. The resulting steep gradients in energy generation cannot be managed with the currently implemented algorithms. A possible solution could be the installation of a weather station in the field test region to improve local measurement by tracking of solar radiation and cloud convection that provide immediate data for the algorithms.

Use Case 1 Application

7.) The successful start of the field test phase and the first results with UC 1 demonstrate that the newly developed ALF-C meets the requirements. As a platform, it will be enhanced for the remaining use cases and its algorithms will be refined based the findings for UC 1.

8.) The local balancing mechanism implemented in the ALF-C, based on a direct control of batteries (15-minutes control cycle), with soft real-time data provision in 15-minutes intervals is able to significantly:

a. Decrease power peaks of the community with the connecting MV-feeder,

b. Decrease the energy exchange,

c. Decrease the amount of energy export and

d. Increase the duration of the uncoupling of a community with the connecting MV-feeder.

Therefore, the principle enables a community to increase the amount of collective self-consumption of locally generated energy and become more self-sufficient, while reducing power peaks at MV-feeder and additional stress on the MV-grid.

9.) The inertia of the battery direct control (15-minutes control cycles) in conjunction of high fluctuating generation by the PV panels can lead to very high positive (export) power peaks at the MV-feeder with an import of energy from the MV-network and consequently have an opposing effect on the targets listed in point 8.

10.) The direct control balancing approach cause very large power flow gradients when the CBES reaches it maximum SOE and stops charging.

11.) The currently implemented local balancing algorithm requires an additional optimization algorithm that enables it to make maximum use of the limited amount of available storage capacity and minimize power peaks. The algorithm has to maximize self-consumption as the main condition and minimize the exchange of power at the local network station as a secondary condition. The optimization requires a forecast of the expected energy generation and demand.

11 List of Tables

12 List of Figures

13 List of References

[1] European Commission, “2050 long-term strategy,” [Online]. Available: https://ec.europa.eu/clima/policies/strategies/2050_en.

[2] “D5.1 Solution Design and Technical Specifications,” Platone EU Horizon 2020 Project, 2020.

[3] “D5.2 Detailed Use Case Descriptions,” Platone EU Horizon 2020 Project, 2020.

[4] “D1.2 Project KPIs definition and measurement methods,” Platone EU Horizon 2020 Project, 2020.

[5] “D9.4 Project Management Plan Version 2,” Platone EU Horizon 2020 Project, 2021.

[6] “D1.3 Overview of regulatory aspects that impact the solution tested in the demos in European Countries,” Platone EU Horizon 2020 Project, 2021.

[7] European Parliament and Council, “Retrieved from Directive (EU) 2018/2001 on the promotion of the use of energy from renewable sources,” 11 12 2018. [Online]. Available: https://eur-lex.europa.eu/legal-content/EN/TXT/?uri=uriserv:OJ.L_.2018.328.01.0082.01.E.

[8] European Parliament and Council, “Directive (EU) 2019/944 on common rules for the internal market for electricity, Article 46,” 2019. [Online]. Available: https://eur-lex.europa.eu/legal-content/EN/TXT/PDF/?uri=CELEX:32019L0944&from=EN.

[9] “D1.1 General functional requirements and specification of joint activities in the demonstrators,” Platone EU Horizon 2020 Project, 2020.

[10] Deutscher Bundestag, “Erneuerbare-Energien-Gesetz,” 2021. [Online]. Available: https://www.gesetze-im-internet.de/eeg_2014/inhalts_bersicht.html.

[11] Deutscher Bundestag, “Energiewirtschaftsgesetz,” 2005. [Online]. Available: https://www.gesetze-im-internet.de/enwg_2005/.

[12] European Parliament and Council,, “Directive 2012/27/EU on energy efficiency,” 25 10 2012. [Online]. Available: https://eur-lex.europa.eu/eli/dir/2012/27/oj.

[13] “D5.3 Definition of Use Case Algorithms,” Platone EU Horizon 2020 Project, 2021.

[14] European Parliament and Council, “Directive (EU) 2018/2001 on the promotion of the use of energy from renewable sources.,” 2018. [Online]. Available: https://eur-lex.europa.eu/legal-content/EN/TXT/?uri=uriserv:OJ.L_.2018.328.01.0082.01.ENG. [Accessed 2021].

14 List of Abbreviations

Abbreviation	Term
ADMS	Advanced Distribution Management System
ALF-C	Avacon Local Flex Controller
BGB	Bürgerliches Gesetzbuch
CBES	Community Battery Energy Storage
CEC	Citizen Energy Community
DER	Distributed Energy Resources
DSO	Related Term
EC	Energy Community
EE	Erneuerbare Energien Gesetz
EMS	Energy Management System
EnWG	Energiewirtschaftsgesetz
EU	European Union
HV	High Voltage
LBES	Local Battery Energy Storage
LEC	Local Energy Community
LV	Low Voltage
MV	Medium Voltage
KPI	Key Performance Indicator
PV	Photovoltaic
REC	Renewable Energy Community
RES	Renewable Energy Sources
SO	System Operator
SOC	State of Charge
SOE	State of Energy
TSO	Transmission System Operator
UC	Use Case
VHV	Very High Voltage
WP	Work Package